Approximation of Axisymmetric Darcy Flow

V.J. Ervin *
Department of Mathematical Sciences
Clemson University
Clemson, SC, 29634-0975
USA.

January 6, 2012

Abstract

In this article we investigate the numerical approximation of the Darcy equations in an axisymmetric domain, subject to axisymmetric data. Rewriting the problem in cylindrical coordinates reduces the 3-D problem to a problem in 2-D. This reduction to 2-D requires the numerical analysis to be studied in suitably weighted Hilbert spaces. In this setting the Raviart-Thomas (RT) and Brezzi-Douglas-Marini (BDM) approximation pairs are shown to be LBB stable, and corresponding a priori error estimates derived. Presented numerical experiments confirm the predicted rates of convergence for the RT and BDM approximations.

Key words. axisymmetric flow; Darcy equation, LBB condition

AMS Mathematics subject classifications. 65N30

1 Introduction

In this article we discuss the numerical approximation of Darcy flow in an axisymmetric domain with axisymmetric data. Our interest in this problem arose from considering the approximation of coupled Stokes-Darcy flow in an axisymmetric domain. Many geometries in nature and from manufacturing are either axisymmetric by evolution or by design. Assuming that the quantities of interest are also axisymmetric, recasting the problem in cylindrical coordinates reduces the problem from a 3-D computational problem to a 2-D computational problem. This reduction significantly reduces the computational effort need to approximate the solution. In addition, axisymmetric computational models are useful in validating more complex 3-D computational models. The starting point for the numerical analysis of coupled Stokes-Darcy flow in an axisymmetric domain is to individually consider Stokes flow and Darcy flow in the axisymmetric setting.

The numerical analysis of the axisymmetric Stokes flow problem has been studied by several researchers. In [22] Ruas showed that for axisymmetric Stokes flow the LBB condition for the stability

*email: vjervin@clemson.edu.

of the approximations was satisfied for: (i) the partition of the domain into quadrilaterals and the $Q_2 - P_1$ velocity-pressure element pair, and (ii) the partition of the domain into triangles (subject to all the triangle having either an edge along, or an edge parallel to, the symmetry axis) and the mini-element velocity-pressure element pair. Belhachmi et al. in [3] showed that the LBB condition was satisfied for the Taylor-Hood $P1isoP2 - P1$ velocity-pressure element pair. A corollary of the LBB condition being satisfied by $P1isoP2 - P1$ elements is that it is also satisfied by the commonly used (for flows in Cartesian coordinates) Taylor-Hood $P2 - P1$ velocity-pressure element pair. One common approach to establishing the stability of the velocity-pressure approximation spaces for Stokes flow is to use the Stenberg criteria [23, 25]. This involves showing that the dimension of the null space of a *local* matrix, generated from a macroelement, is one. In [13] we showed that the Stenberg criteria extended to the axisymmetric setting and gave an easy proof of the stability of the Taylor-Hood $P2 - P1$ velocity-pressure element pair, and for the Crouzeix-Raviart approximation pair. Recently Lee and Li, in [17], showed the stability of the family of Taylor-Hood approximation pairs for this problem. Unlike the previous work where the analysis was done in the axisymmetric domain, Lee and Li performed their analysis in a 3-D setting. A more general problem, that of approximating the Stokes equations in an axisymmetric domain, was studied by Belhachmi et al. in [4].

We are not aware of any papers which present the analysis of the mixed formulation of axisymmetric Darcy flow. (In [18], building upon the work in [5, 3] Li studied the approximation of the Poisson problem in an axisymmteric domain, in particular, the use of appropriately graded meshed for singular solutions. The Darcy flow equations also arise as a mixed method formulation to the Poisson problem.) Commonly used elements for the velocity and pressure approximation of Darcy equations in the Cartesian coordinate setting are the Raviart-Thomas pairs ($RT_k - discP_k$) and the Brezzi-Douglas-Marini pairs ($BDM_{k+1} - discP_k$) [9] . With these choices the velocity and pressure approximation spaces, X_h and Q_h, satisfy $div(X_h) = Q_h$. With this property the L^2 coercivity of $a(\mathbf{u}, \mathbf{v}) = \int_\Omega \nu\, \mathbf{u} \cdot \mathbf{v}\, d\mathbf{x}$ on $Z_h = \{\mathbf{v} \in X_h : \int_\Omega q \nabla \cdot \mathbf{v} = 0\,,\ \forall q \in Q_h\}$ establishes the desired H_{div} coercivity on Z_h. The property $div(X_h) = Q_h$ also results in the very attractive property that the computed approximation for the velocity is pointwise div-free, i.e. the approximation conserves mass pointwise.

In the axisymmetric setting for RT and BDM elements the property $div_{axi}(X_h) = Q_h$ does not hold. In fact the operator div_{axi} does not map a (vector) polynomial velocity space into a (scalar) polynomial space.

In the Cartesian setting the RT elements have the property that for ρ the associated interpolation operator and Π the L^2 projection operator, one has that

$$\|div\mathbf{v} - div\rho(\mathbf{v})\| = \|(I - \Pi)\, div\mathbf{v}\|\,. \tag{1.1}$$

This property is often illustrated pictorially and referred to as the commuting property diagram [9]. It is this property that permits the divergence of a function to be computed to the same order of accuracy as the function itself when using a RT approximation. In the axisymmetric setting the direct analog of (1.1) does not hold.

Additionally, because of the different operators and norms involved, the stability of RT and BDM approximation (i.e. that RT and BDM elements satisfy the LBB condition) in the Cartesian setting does not guarantee stability of the approximations in the axisymmetric setting.

The typical approach to obtaining the a priori error estimate is to map each element, T, in the par-

tition $\mathcal{T}_h$, of the domain to a reference element, $\widehat{T}$, apply approximation properties on the reference element, and then map back to the element. In the axisymmetric setting, because of the weighted norms, the approximation constants arising from applying the approximation properties on $\widehat{T}$ depend on T. Two different approaches were used by Belhachmi et al. in [3], and Lee and Li in [17], to establish the accuracy of the discrete approximation in the axisymmetric Stokes problem. In [3] the authors established their results by generalizing results for the Clément approximation operator to weighted norms. In [17] the error analysis was done by using interpolating results in the 3-D setting. As we are using different approximation spaces for the velocity (discontinuous) and different norms the results of [3, 17] are not directly application to the RT and BDM approximations of the axisymmetric Darcy flow problem.

The paper is organized as follows. In the following section we present the axisymmetric Darcy flow problem, introduce the appropriate function space setting, give the corresponding weak formulation, and describe the setting for the finite element approximation. Section 3 contains the analysis of the finite element approximation of the axisymmetric Darcy flow problem, using $RT_k - discP_k$ and $BDM_{k+1} - discP_k$ approximating elements. At the beginning of this section we presents the definition of RT_k and BDM_k for the axisymmetric setting and establishes a commuting diagram property. Also, we show that approximation constants which arises from applying the approximation properties on $\widehat{T}$ are uniformly bounded. Two approaches are used to establish computability of the finite element approximation. In Subsection 3.1, borrowing an idea from the approximation of the Navier-Stokes equations, we apply grad-div stabilization to the Darcy equation in order to guarantee coercivity of the appropriate bilinear form. Stability of the $RT_k - discP_k$ and $BDM_{k+1} - discP_k$ approximations are then established by extending the Stenberg criteria to the current setting. A priori error estimates for the approximation are also presented. In Subsection 3.2 we use mesh dependent norms for the velocity and pressure spaces in order to establish the computability of the approximation without applying grad-div stabilization. Again, stability of the approximation is established by extending the Stenberg criteria, and a priori error estimates presented. Numerical experiments are given in Section 4, and the computation results for the approximation errors compared to those predicted theoretically.

2 Axisymmetric Darcy Equations

In this section we give the mathematical framework for modeling axisymmetric Darcy flow and discuss the existence and uniqueness of the solution.

2.1 Problem Description

Let $\breve{\Omega} \subset \mathbb{R}^3$ denote a domain formed as a volume of revolution about the z-axis. With respect to cylinderical coordinates, (r, θ, z), let Ω denote the half section of $\breve{\Omega}$, $\Omega := \breve{\Omega} \cap \{(r, 0, z) : r > 0, z \in \mathbb{R}\}$. For the description of the boundary let $\Gamma := \partial\breve{\Omega} \cap \partial\Omega$, and Γ_0 the intersection of $\breve{\Omega}$ and the z-axis, $\Gamma_0 := \breve{\Omega} \cap \{(0, 0, z) : z \in \mathbb{R}\}$. Note that $\partial\Omega = \Gamma \cup \Gamma_0$. In addition, assume that Ω is a simply connected domain with a polygonal boundary. (See Figure 2.1.)

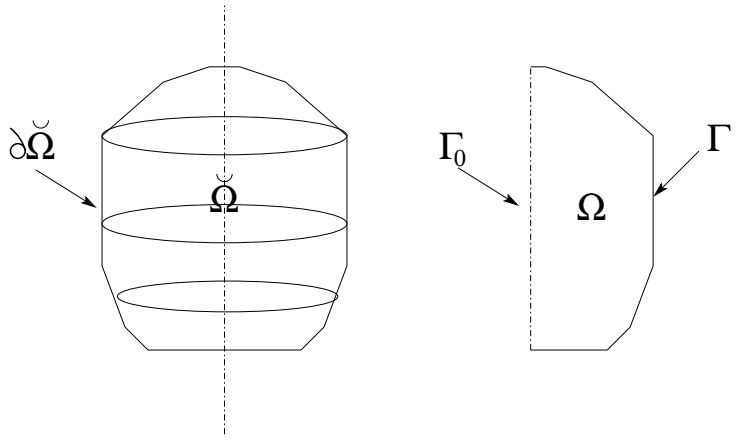

Figure 2.1: Illustration of axisymmetric flow domain.

Consider Darcy equations (in Cartesian coordinates) in $\breve{\Omega}$:

$$\mu\breve{\mathbf{K}}^{-1}\breve{\mathbf{u}} + \nabla\breve{p} = \breve{\mathbf{f}} \quad \text{in } \breve{\Omega}, \tag{2.1}$$

$$\nabla\cdot\breve{\mathbf{u}} = \breve{s} \quad \text{in } \breve{\Omega}, \tag{2.2}$$

$$\breve{\mathbf{u}}\cdot\breve{\mathbf{n}} = \breve{g} \quad \text{on } \partial\breve{\Omega}, \tag{2.3}$$

where $\breve{\mathbf{u}} = \begin{bmatrix} u_x \\ u_y \\ u_z \end{bmatrix} = u_x\mathbf{e}_x + u_y\mathbf{e}_y + u_z\mathbf{e}_z$, for $\mathbf{e}_x$, $\mathbf{e}_y$, $\mathbf{e}_z$ denoting unit vectors in the x, y and z directions, respectively. In (2.1)-(2.3) $\breve{\mathbf{u}}$ denotes the fluid's velocity, $\breve{p}$ the pressure, $\breve{\mathbf{f}}$ an external forcing function, $\breve{s}$ a fluid sink/source term, $\breve{g}$ the fluid outflow along the boundary, μ the fluid viscosity, and $\breve{\mathbf{K}}$ the permeability (symmetric, positive definite) tensor of the domain. Additionally, associated with (2.1)-(2.3) is the compatiablity condition $\int_{\breve{\Omega}}\breve{s}\,dV = \int_{\partial\breve{\Omega}}\breve{g}\,dS$. We assume that the data $\breve{\mathbf{f}}$, $\breve{s}$, $\breve{g}$ are axisymmetric, giving rise to an axisymmetric solution ($\breve{\mathbf{u}}$, $\breve{p}$) [5].

For simplicity, assume that $\breve{s} = 0$, $\breve{g} = 0$, $\breve{\mathbf{K}} = k\mathbf{I}$, where $k > 0$ is a constant, and $\nu := \mu/k$. (The assumption $\breve{s} = 0$, $\breve{g} = 0$ i.e. equivalent to introducing a change of variable $\breve{\mathbf{u}} = \breve{\mathbf{u}}_0 + \breve{\mathbf{u}}_p$, where $\breve{\mathbf{u}}_p = \nabla w$ and w satisfies $\nabla\cdot\nabla w = \breve{s}$ in $\breve{\Omega}$, $\partial w/\partial\breve{\mathbf{n}} = \breve{g}$ on $\partial\breve{\Omega}$.)

Multiplying (2.1) through by a suitable smooth function $\breve{\mathbf{v}}$, $\breve{\mathbf{v}}\cdot\breve{\mathbf{n}}|_{\partial\breve{\Omega}} = \mathbf{0}$ and integrating over $\breve{\Omega}$, and multiplying (2.2) through by a suitable smooth function q and integrating over $\breve{\Omega}$ we obtain

$$\int_{\breve{\Omega}}\nu\breve{\mathbf{u}}\cdot\breve{\mathbf{v}}\,dV - \int_{\breve{\Omega}}\breve{p}\nabla\cdot\breve{\mathbf{v}}\,dV = \int_{\breve{\Omega}}\breve{\mathbf{f}}\cdot\breve{\mathbf{v}}\,dV \tag{2.4}$$

$$\int_{\breve{\Omega}}\breve{q}\nabla\cdot\breve{\mathbf{u}}\,d\mathbf{x} = 0\ . \tag{2.5}$$

Expressing $\breve{\mathbf{u}}$ in cylinderical coordinates, $\breve{\mathbf{u}} = \begin{bmatrix} u_r \\ u_\theta \\ u_z \end{bmatrix} = u_r\mathbf{e}_r + u_\theta\mathbf{e}_\theta + u_z\mathbf{e}_z$, and as the flow is axisymmetric, i.e. $\breve{\mathbf{u}}(r,\theta,z) = \mathbf{u}(r,z)$, $\breve{\mathbf{f}}(r,\theta,z) = \mathbf{f}(r,z)$, $\breve{p}(r,\theta,z) = p(r,z)$, $u_r(0,z) = 0$, $u_\theta(0,z) =$

0, equations (2.4)(2.5) transform into

$$\int_\Omega \nu\, \mathbf{u}\cdot\mathbf{v}\, r\, d\mathbf{x} \;-\; \int_\Omega p\, \nabla_a\cdot\mathbf{v}\, r\, d\mathbf{x} \;-\; \int_\Omega p\, v_r\, d\mathbf{x} \;=\; \int_\Omega \mathbf{f}\cdot\mathbf{v}\, r\, d\mathbf{x}\,, \tag{2.6}$$

$$\int_\Omega \nu\, u_\theta\, v_\theta\, r\, d\mathbf{x} \;=\; \int_\Omega f_\theta\, v_\theta\, r\, d\mathbf{x}\,, \tag{2.7}$$

$$\int_\Omega q\, \nabla_a\cdot\mathbf{u}\, r\, d\mathbf{x} \;+\; \int_\Omega q\, u_r\, d\mathbf{x} \;=\; 0\,, \tag{2.8}$$

$$\text{where}\quad \mathbf{u}=\begin{bmatrix} u_r\\ u_z\end{bmatrix},\ \mathbf{v}=\begin{bmatrix} v_r\\ v_z\end{bmatrix},\ \mathbf{f}=\begin{bmatrix} f_r\\ f_z\end{bmatrix},\ \nabla_a:=\begin{bmatrix} \partial/\partial r\\ \partial/\partial z\end{bmatrix},\quad \text{and}\quad d\mathbf{x}:=dr\,dz\,.$$

Note that the angular flow equation for u_θ is decoupled from the flow equations for u_r and u_z. For simplicity assume $u_\theta = 0$.

2.2 Function Spaces and Weak Formulation

Let Θ denote a domain in $\mathbb{R}^2$. For any real α and $1 \le p < \infty$, the space ${}_\alpha L^p(\Theta)$ is defined as the set of measurable functions w such that

$$\|w\|_{{}_\alpha L^p(\Theta)} \;:=\; \left(\int_\Theta |w|^p\, r^\alpha\, d\mathbf{x}\right)^{1/p} < \infty\,, \tag{2.9}$$

where $r = r(\mathbf{x})$ is the radial coordinate of $\mathbf{x}$, i.e. the distance of a point $\mathbf{x}$ in Θ from the symmetry axis. The subspace ${}_1L^2_0(\Theta)$ of ${}_1L^2(\Theta)$ denotes the functions q with weighted integral equal to zero:

$$\int_\Theta q\, r\, d\mathbf{x} \;=\; 0\,.$$

Define the weighted Sobolev space ${}_1W^{l,p}(\Theta)$ as the space of functions in ${}_1L^p(\Theta)$ such that their partial derivatives of order less that or equal to l belong to ${}_1L^p(\Theta)$. Associated with ${}_1W^{l,p}(\Theta)$ is the semi-norm $|\cdot|_{{}_1W^{l,p}(\Theta)}$ and norm $\|\cdot\|_{{}_1W^{l,p}(\Theta)}$ defined by

$$|w|_{{}_1W^{l,p}(\Theta)} \;=\; \left(\sum_{k=0}^{l} \|\partial_r^k\partial_z^{l-k} w\|^p_{{}_1L^p(\Theta)}\right)^{1/p}, \qquad \|w\|_{{}_1W^{l,p}(\Theta)} \;=\; \left(\sum_{k=0}^{l} |w|^p_{{}_1W^{k,p}(\Theta)}\right)^{1/p}.$$

When $p = 2$, we denote ${}_1W^{l,2}(\Theta)$ as ${}_1H^l(\Theta)$.

For $\mathbf{v}=\begin{bmatrix} v_r\\ v_z\end{bmatrix}$, let

$$div_{axi}(\mathbf{v}) \;:=\; \nabla_a\cdot\mathbf{v} + \frac{v_r}{r}\,, \quad \text{and} \quad {}_1H^{div_{axi}}(\Theta) \;:=\; \left\{\mathbf{v}\in \left({}_1L^2(\Theta)\right)^2 \,:\, div_{axi}(\mathbf{v}) \in {}_1L^2(\Theta)\right\}. \tag{2.10}$$

In order to incorporate the boundary condition $\mathbf{u}\cdot\mathbf{n} = 0$ on Γ, and because of axisymmetry, let

$${}_1H^{div_{axi}}_0(\Omega) \;:=\; \left\{\mathbf{v}\in {}_1H^{div_{axi}}(\Omega) \,:\, \mathbf{v}\cdot\mathbf{n} \,=\, 0 \ \text{ on } \ \partial\Omega\right\}. \tag{2.11}$$

Let $X := {}_1H_0^{div_{axi}}(\Omega)$ and for $\mathbf{v} = [v_r, v_z]^T$,

$$\|\mathbf{v}\|_{X(\Theta)} = \left(\|v_r\|^2_{{}_1L^2(\Theta)} + \|v_z\|^2_{{}_1L^2(\Theta)} + \|div_{axi}(\mathbf{v})\|^2_{{}_1L^2(\Theta)}\right)^{1/2},$$

and $Q := {}_1L^2_0(\Omega)$ with $\|\cdot\|_Q = \|\cdot\|_{{}_1L^2(\Omega)}$. When $\Theta = \Omega$, $\|\mathbf{v}\|_X := \|\mathbf{v}\|_{X(\Theta)}$. With X we associate the innerproduct

$$\langle \mathbf{v}, \mathbf{w}\rangle_X := \int_\Omega (\mathbf{v}\cdot\mathbf{w} + div_{axi}(\mathbf{v}) div_{axi}(\mathbf{w}))\, r\, d\mathbf{x}\,. \tag{2.12}$$

Using as the pivot space $\left({}_1L^2(\Omega)\right)^2$ with innerproduct $\langle \mathbf{f}, \mathbf{g}\rangle := \int_\Omega \mathbf{f}\cdot\mathbf{g}\, r\, d\mathbf{x}$, let X^* denote the dual space of X, i.e. X^* is the completion of $\left({}_1L^2(\Omega)\right)^2$ with respect to the norm

$$\|\mathbf{f}\|_{X^*} = \sup_{\mathbf{g}\in X} \frac{\langle \mathbf{f}, \mathbf{g}\rangle}{\|\mathbf{g}\|_X}\,.$$

For Θ a domain in $\mathbb{R}^n$, $n = 2, 3$, we use the standard definitions for $L^2(\Theta)$, $L^2_0(\Theta)$, $H^k(\Theta)$, and $H^k_0(\Theta)$ (see [1]).

The weak axisymmetric formulation for the Darcy equations can be stated as: *Given* $\mathbf{f} \in X^*$, *determine* $(\mathbf{u}, p) \in (X \times Q)$ *satisfying*

$$a(\mathbf{u}, \mathbf{v}) - b_a(p, \mathbf{v}) = \langle \mathbf{f}, \mathbf{v}\rangle_{X^*,X} \quad \forall \mathbf{v} \in X\,, \tag{2.13}$$

$$b_a(q, \mathbf{u}) = 0\,, \quad \forall q \in Q\,, \tag{2.14}$$

where

$$a(\mathbf{u}, \mathbf{v}) := \int_\Omega \nu\, \mathbf{u}\cdot\mathbf{v}\, r\, d\mathbf{x}\,, \tag{2.15}$$

$$b_a(q, \mathbf{v}) := \int_\Omega q\, \nabla_a\cdot\mathbf{v}\, r\, d\mathbf{x} + \int_\Omega q\, v_r\, d\mathbf{x}\,, \tag{2.16}$$

and $\langle\cdot,\cdot\rangle_{X^*,X}$ denotes the duality pairing between X and X^*.

2.3 Existence and Uniqueness of $(\mathbf{u}\,, p)$ satisfying (2.13)(2.14)

The existence and uniqueness of the solution to (2.13)(2.14) follows from that for Darcy equations in $\mathbb{R}^3$ (in Cartesian coordinates), and the uniqueness of the transformation of the axisymmetric problem in $\mathbb{R}^3$ to (2.13)(2.14). (See [5, 3] for an analogous discussion for the axisymmetric Stokes problem.) In particular we note that there exists $\beta > 0$ such that

$$\inf_{q\in Q}\sup_{\mathbf{v}\in X} \frac{b_a(q, \mathbf{v})}{\|q\|_Q\, \|\mathbf{v}\|_X} \geq \beta\,. \tag{2.17}$$

3 Finite Element Approximation

We assume that Ω is a convex polygonal domain and $(\mathcal{T}_h)_h$ denotes a family of uniformly regular triangulations of Ω satisfying:

(i) The domain $\overline{\Omega}$ is the union of the triangles of $\mathcal{T}_h$.

(ii) $T_k \cap T_j$ is a side, a node, or empty for all triangles T_k, T_j, $k \neq j$, in $\mathcal{T}_h$.

(iii) There exists a constant σ, independent of h, such that for all $T \in \mathcal{T}_h$ its diameter h_T is smaller that h and T contains a circle of radius $\sigma\, h_T$.

Additionally we assume that each triangle T in $\mathcal{T}_h$ has at least one vertex inside Ω (i.e. not on $\Gamma \cap \Gamma_0$).

For $X_h \subset X$, $Q_h \subset Q$, an approximation to (2.13)(2.14) may be stated as: *Given* $\mathbf{f} \in X^*$, *determine* $(\mathbf{u}_h,\, p_h) \in (X_h \times Q_h)$ *satisfying*

$$\begin{aligned} a(\mathbf{u}_h,\, \mathbf{v}) \; - b_a(p_h,\, \mathbf{v}) \;\; &= \;\; \langle \mathbf{f}, \mathbf{v} \rangle_{X^*,X} \quad \forall \mathbf{v} \in X_h \,, && (3.1) \\ b_a(q,\, \mathbf{u}_h) \;\; &= \;\; 0 \;, \quad \forall q \in Q_h \,. && (3.2) \end{aligned}$$

As with the continuous formulation, the solvability of (3.1)(3.2) for $(\mathbf{u}_h,\, p_h)$ is contingent on the discrete approximation spaces satisfying, for some $\beta > 0$, the discrete LBB condition

$$\inf_{q \in Q_h} \sup_{\mathbf{v} \in X_h} \frac{b_a(q,\, \mathbf{v})}{\|q\|_Q \, \|\mathbf{v}\|_X} \;\geq\; \beta \,. \tag{3.3}$$

Two commonly used approximation *pairs* for Darcy flow in the Cartesian formulation are Raviart-Thomas $RT_k - discP_k$, and Brezzi-Douglas-Marini $BDM_k - discP_{k-1}$. Next we show that with minor modification these approximation pairs are also LBB stable for the axisymmetric formulation.

For $\Theta \subset \overline{\Omega}$, denote by $P_k(\Theta)$, $\tilde{P}_k(\Theta)$, $k \in \mathbb{N} \cup \{0\}$, the set of polynomials of degree $\leq k$, and the set of homogeneous polynomials of degree k on Θ, respectively. Additionally, let $\mathcal{E}(\Theta)$ denote the set of edges in the triangulation $\mathcal{T}_h$ in Θ, and

$$R_k(\partial T) \;:=\; \{\phi \in L^2(\partial T) \;:\; \phi|_e \in P_k(e) \;,\; e \in \mathcal{E}(T)\} \,.$$

For $\Omega \subset \mathbb{R}^2$, $T \in \mathcal{T}_h$, the Raviart-Thomas space, $RT_k(T)$, is defined by

$$RT_k(T) \;:=\; (P_k(T))^2 \;+\; \begin{bmatrix} r \\ z \end{bmatrix} \tilde{P}_k(T) \,, \tag{3.4}$$

where, for $\mathbf{q} \in RT_k(T)$, $\mathbf{n}$ the unit outer normal on ∂T, the degrees of freedom are given by

$$\int_{\mathcal{E}(T)} \mathbf{q} \cdot \mathbf{n}\, p \, ds \,, \quad p \in R_k(\partial T) \,, \quad \text{and} \quad \int_T \mathbf{q} \cdot \mathbf{p} \, d\mathbf{x} \,, \quad \mathbf{p} \in (P_{k-1}(T))^2 \;. \tag{3.5}$$

For the axisymmetric formulation we redefine $\mathcal{E}(\Theta)$ as the set of edges in $\mathcal{T}_h$ lying in Θ which <u>do not</u> lie along the symmetry axis Γ_0, $\mathcal{E}(\mathcal{T}_h) := \cup_{T \in \mathcal{T}_h} \mathcal{E}(T)$, and define

$$RT_k^{axi}(T) \;:=\; \{\mathbf{q} \in RT_k(T) \;:\; \mathbf{q} \cdot \mathbf{n}|_{\Gamma_0} \;=\; 0\} \;=\; \left\{ \begin{bmatrix} q_r \\ q_z \end{bmatrix} \in RT_k(T) \;:\; q_r|_{\Gamma_0} \;=\; 0 \right\} , \tag{3.6}$$

where the degrees of freedom are given by

$$\int_{\mathcal{E}(T)} \mathbf{q}\cdot\mathbf{n}\, p\, r\, ds\,, \quad p \in R_k(\partial T)\,, \quad \text{and} \quad \int_T \mathbf{q}\cdot\mathbf{p}\, r\, d\mathbf{x}\,, \quad \mathbf{p} \in (P_{k-1}(T))^2\,. \tag{3.7}$$

The unique solvability of $\mathbf{q} \in RT_k^{axi}(T)$ in terms of the degrees of freedom (3.7) follows as in the Cartesian case [9, 15].

The Brezzi-Douglas-Marini space, $BDM_k(T)$, is defined by $BDM_k(T) := (P_k(T))^2$. For the axisymmetric setting, we define

$$BDM_k^{axi}(T) := \{\mathbf{q} \in BDM_k(T) : \mathbf{q}\cdot\mathbf{n}|_{\Gamma_0} = 0\} = \left\{ \begin{bmatrix} q_r \\ q_z \end{bmatrix} \in BDM_k(T) : q_r|_{\Gamma_0} = 0 \right\}. \tag{3.8}$$

The associated degrees of freedom are given by

$$\int_{\mathcal{E}(T)} \mathbf{q}\cdot\mathbf{n}\, p\, r\, ds\,, \quad p \in R_k(\partial T)\,, \qquad \int_T \mathbf{q}\cdot\nabla_a p\, r\, d\mathbf{x}\,, \quad p \in P_{k-1}(T)\,, \tag{3.9}$$

$$\text{and} \qquad \int_T \mathbf{q}\cdot\mathbf{curl}(b_T\, p)\, r\, d\mathbf{x}\,, \quad p \in P_{k-2}(T)\,, \tag{3.10}$$

where b_T denotes the cubic bubble function on T.

The unique solvability of $\mathbf{q} \in BDM_k^{axi}(T)$ in terms of the degrees of freedom (3.9)(3.10) follows as in the Cartesian case [9].

The local interpolation operators are defined in an analogous manner. Specifically, for $RT_k^{axi}(T)$ the local interpolation operator ρ_T is defined as follows. For $s > 2$, let

$$\rho_T : {}_1H^{div_{axi}}(T) \cap {}_1L^s(T) \longrightarrow RT_k^{axi}(T)\,, \tag{3.11}$$

be defined by

$$\int_{\mathcal{E}(T)} (\mathbf{q} - \rho_T\mathbf{q})\cdot\mathbf{n}\, p\, r\, ds = 0\,, \quad p \in R_k(\partial T)\,, \tag{3.12}$$

$$\int_T (\mathbf{q} - \rho_T\mathbf{q})\cdot\mathbf{p}\, r\, d\mathbf{x} = 0\,, \quad \mathbf{p} \in (P_{k-1}(T))^2\,. \tag{3.13}$$

Note that, from the uniqueness of the interpolant, if $\mathbf{q} \in RT_k^{axi}(T)$ then $\rho_T\mathbf{q} = \mathbf{q}$.

Let $RT_k^{axi}(\mathcal{T}_h) := \cup_{T\in\mathcal{T}_h} RT_k^{axi}(T)$, and define the global interpolation operator $\rho_h : {}_1H^1(\Omega) \longrightarrow RT_k^{axi}(\mathcal{T}_h)$ as

$$\rho_h(\mathbf{q})|_T := \rho_T(\mathbf{q}|_T)\,, \quad \forall T \in \mathcal{T}_h\,. \tag{3.14}$$

Similar to the Cartesian case we have a *commuting diagram property*. Note that div_{axi} does not map a (vector) polynomial space to a (scalar) polynomial space.

Let $\pi_k : {}_1L^2(T) \longrightarrow P_k(T)$ denote the projection operator defined by

$$\int_T (w - \pi_k(w))\, p\, r\, d\mathbf{x} = 0\,, \quad \forall p \in P_k(T)\,. \tag{3.15}$$

Lemma 1 *With ρ_T and π_k defined above, for $\mathbf{q} \in {}_1H^{div_{axi}}(T) \cap {}_1L^s(T)$,*

$$\pi_k div_{axi} \rho_T(\mathbf{q}) \;=\; \pi_k div_{axi} \mathbf{q}\,. \tag{3.16}$$

Note that (3.16) is equivalent to the *commuting diagram property* illustrated in Figure 3.1.

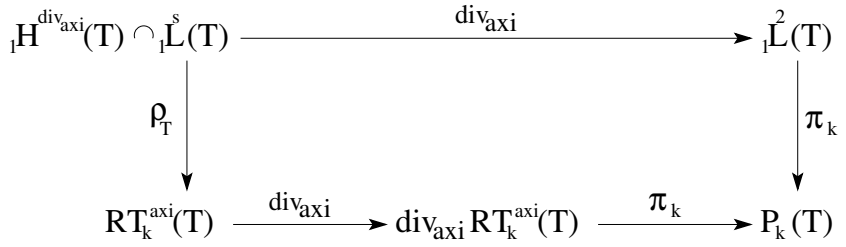

Figure 3.1: Commuting diagram property.

Proof Let $p \in P_k(T)$. Then,

$$\begin{aligned}
\int_T p\, \pi_k div_{axi} \mathbf{q}\, r\, d\mathbf{x} \;-\; \int_T p\, \pi_k div_{axi} \rho_T(\mathbf{q})\, r\, d\mathbf{x} \;&=\; \int_T p\, div_{axi}\, (\mathbf{q} \,-\, \rho_T(\mathbf{q}))\; r\, d\mathbf{x} \\
&= \int_T p\, \nabla_a \cdot r\; (\mathbf{q} \,-\, \rho_T(\mathbf{q}))\; d\mathbf{x} \\
&= \int_{\partial T} (\mathbf{q} \,-\, \rho_T(\mathbf{q})) \cdot \mathbf{n}\, p\, r\, ds \;-\; \int_T (\mathbf{q} \,-\, \rho_T(\mathbf{q})) \cdot \nabla_a p\; r\, d\mathbf{x} \\
&= 0\,, \quad \text{using properties (3.12),(3.13).}
\end{aligned}$$

■

For $BDM_k^{axi}(T)$, $s > 2$, the local interpolation operator $\tilde{\rho}_T \,:\, {}_1H^{div_{axi}}(T) \cap {}_1L^s(T) \longrightarrow BDM_k^{axi}(T)$, is defined by

$$\int_{\mathcal{E}(T)} (\mathbf{q} \,-\, \tilde{\rho}_T \mathbf{q}) \cdot \mathbf{n}\, p\, r\, ds\,, \quad p \in R_k(\partial T)\,, \qquad \int_T (\mathbf{q} \,-\, \tilde{\rho}_T \mathbf{q}) \cdot \nabla_a p\, r\, d\mathbf{x}\,, \quad p \in P_{k-1}(T)\,, \tag{3.17}$$

$$\text{and} \qquad \int_T (\mathbf{q} \,-\, \tilde{\rho} \mathbf{q}) \cdot \mathbf{curl}(b_T\, p)\, r\, d\mathbf{x}\,, \quad p \in P_{k-2}(T) \tag{3.18}$$

and the global interpolation operator $\tilde{\rho}_h \,:\, {}_1H^1(\Omega) \longrightarrow BDM_k^{axi}(\mathcal{T}_h)$ defined as

$$\tilde{\rho}_h(\mathbf{q})|_T \;:=\; \tilde{\rho}_T(\mathbf{q}|_T)\,, \quad \forall T \in \mathcal{T}_h\,. \tag{3.19}$$

Analogous to Lemma 1 we having a *commuting diagram property.*

Lemma 2 *With $\tilde{\rho}_T$ and π_{k-1} defined above, for $\mathbf{q} \in {}_1H^{div_{axi}}(T) \cap {}_1L^s(T)$,*

$$\pi_{k-1} div_{axi} \tilde{\rho}_T(\mathbf{q}) \;=\; \pi_{k-1} div_{axi} \mathbf{q}\,. \tag{3.20}$$

■

Before presenting the estimate for the local interpolation error we recall the Piola transformation and several properties.

For $T \in \mathcal{T}_h$, (see Figure 3.2) let

$$F_T(\boldsymbol{\xi}) = \begin{bmatrix} F_{T_r}(\boldsymbol{\xi}) \\ F_{T_z}(\boldsymbol{\xi}) \end{bmatrix} = J_T\boldsymbol{\xi} + \begin{bmatrix} r_1 \\ z_1 \end{bmatrix}, \quad J_T = \begin{bmatrix} (r_2 - r_1) & (r_3 - r_1) \\ (z_2 - z_1) & (z_3 - z_1) \end{bmatrix}, \text{ and } |J_T| = |detJ_T|\,. \tag{3.21}$$

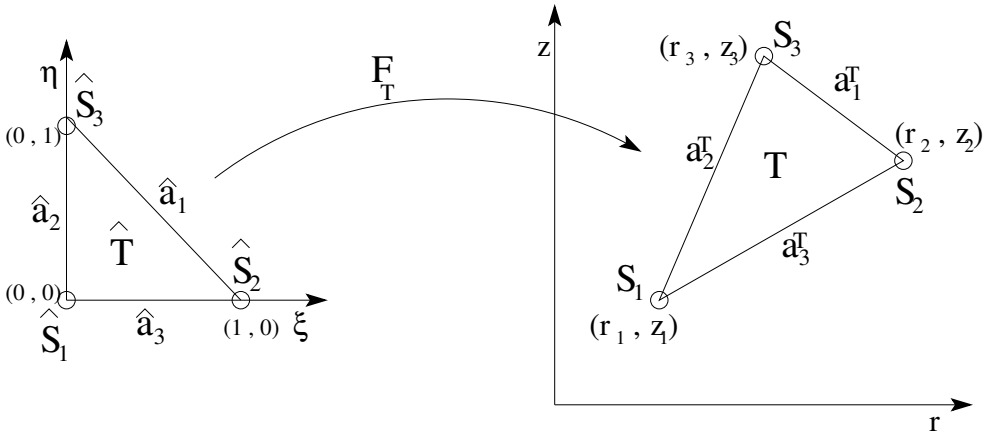

Figure 3.2: Mapping of triangle T to the reference triangle $\widehat{T}$.

For a scalar function $g : T \longrightarrow \mathbb{R}$, let $\hat{g} = g \circ F_T$. In particular, $\hat{r} = r \circ F_T$.

The Piola transformation $\mathcal{P} : L^2(\widehat{T}) \longrightarrow T$ is defined by

$$\hat{\mathbf{q}} \longmapsto \mathbf{q}(x) = \mathcal{P}(\hat{\mathbf{q}})(x) := \frac{1}{|J_T|} J_T \hat{\mathbf{q}}(\hat{x})\,. \tag{3.22}$$

Because of the r terms which appears in the integrals in the (r, z) space we introduce the following norm definition in order to relate norms over T to norms over $\widehat{T}$. (Compare with (2.9).) For $\hat{w} = w \circ F_T$,

$$\left\|\left|\hat{w}\right|\right\|_{\alpha L^p(T)} = \left(\int_{\widehat{T}} |\hat{w}|^p \, \hat{r}^\alpha \, d\boldsymbol{\xi} \right)^{1/p}. \tag{3.23}$$

Norms $\|\|\cdot\|\|_{{}_1W^{k,p}(T)}$ and associated semi-norms, $\|\|\cdot|\|_{{}_1W^{k,p}(T)}$, are similarly defined. For a square matrix B, $\|B\|$ denotes the 2-norm of B.

Lemma 3 *(See [11, 9]) For $v \in {}_1H^m(T)$, $\hat{v} := v \circ F_T$, $\mathbf{q} \in {}_1H^m(T)$, $\hat{\mathbf{q}} := \mathcal{P}^{-1}(\mathbf{q})$, we have that there exists $C > 0$ (depending on m) such that*

$$\|v\|_{{}_1H^m(T)} \leq C\,|J_T|^{1/2}\,\|J_T^{-1}\|^m\,\left\|\left|\hat{v}\right|\right\|_{{}_1H^m(T)}\,, \tag{3.24}$$

$$\left\|\left|\hat{v}\right|\right\|_{{}_1H^m(T)} \leq C\,|J_T|^{-1/2}\,\|J_T\|^m\,\|v\|_{{}_1H^m(T)}\,, \tag{3.25}$$

$$\|\mathbf{q}\|_{{}_1H^m(T)} \leq |J_T|^{-1/2}\,\|J_T^{-1}\|^m\,\|J_T\|\,\left\|\left|\hat{\mathbf{q}}\right|\right\|_{{}_1H^m(T)}\,, \tag{3.26}$$

$$\left\|\left|\hat{\mathbf{q}}\right|\right\|_{{}_1H^m(T)} \leq |J_T|^{1/2}\,\|J_T\|^m\,\|J_T^{-1}\|\,\|\mathbf{q}\|_{{}_1H^m(T)}\,, \tag{3.27}$$

Proof As in the Cartesian case, we have that

$$\nabla_a \mathbf{q} \;=\; \frac{1}{|J_T|} J_T \, \nabla_{\hat{a}} \hat{\mathbf{q}} \, J_T^{-1}\,, \quad \text{and} \quad \nabla_a \cdot \mathbf{q} \;=\; \frac{1}{|J_T|} \nabla_{\hat{a}} \cdot \hat{\mathbf{q}}\,.$$

The above properties can be verified by direct computation.

■

To establish the interpolation error estimate we use the fact that the interpolation operator acts as the identity operator on polymonial of degree $\leq k$, and apply the Bramble-Hilbert Lemma. To account for the different shape and size triangles the analysis is done by mapping the triangle T to the the reference triangle $\widehat{T}$, via (3.21),(3.22), using the Bramble-Hilbert Lemma, and then mapping back to T. The Bramble-Hilbert Lemma uses the following result.

Theorem 1 *[11] There exists a constant $C(\Theta)$ such that*

$$\forall v \in W^{k+1,p}(\Theta)\,, \qquad \inf_{p \in P_k(\Theta)} \|v+p\|_{W^{k+1,p}(\Theta)} \;\leq\; C(\Theta)\, |v|_{W^{k+1,p}(\Theta)}\,. \tag{3.28}$$

In the case we are considering (3.28) holds for *norms* $|||\cdot|||_{_1 W^{k,p}(T)}$ and associated semi-norms, $||\cdot||_{_1 W^{k,p}(T)}$. However the constant $C(\Theta)$ in (3.28), though not dependent on v, depends upon the norm. Mapping each triangle T to $\widehat{T}$ provides a different norm and consequently a different constant $C_T(\widehat{T})$. In order to obtain an interpolation error estimate for Ω independent of $\mathcal{T}_h$ we need to establish that there exists a $C(\widehat{T})$ such that $C_T(\widehat{T}) \;\leq\; C(\widehat{T})\,, \quad \forall T \in \mathcal{T}_h$. We do this by considering the triangles $T \in \mathcal{T}_T$ partitioned into three different cases.

By assumption of a regular triangulation, there exists constants c_J, $C_J > 0$ such that

$$c_J h_T^2 \;\leq\; |det(J_T)| \;=\; |J_T| \;\leq\; C_J h_T^2\,.$$

For $\Theta \subset \Omega$, let $r_{max}(\Theta) := max\{r : (r,\, z) \in \bar{\Theta}\}$, and $r_{min}(\Theta) := min\{r : (r,\, z) \in \bar{\Theta}\}$.

For constants c_1, c_2, $c_3 > 0$ the following inequalities hold.

Type 1: $T \cap \Gamma_0$ is empty. For these triangles we have that

$$r_{min}(T) \;\geq\; c_1\, h_T\,, \quad r_{max}(T) \;\leq\; c_2\, r_{min}(T)\,. \tag{3.29}$$

Type 2: $T \cap \Gamma_0$ is a side. For these triangles we assume that the local counter-clockwise labeling of T is such that the vertices S_1 and S_3 (equivalently a_2^T) lie on Γ_0. Then, for $\hat{r} = r \circ F_T$, we have

$$\hat{r} \;=\; r_2\, \xi \;=\; r_{max}(T)\, \xi\,. \tag{3.30}$$

Type 3: $T \cap \Gamma_0$ is a point. For these triangles we assume that the local counter-clockwise labeling of T is such that the vertex S_1 lies on Γ_0. Then, for $\hat{r} = r \circ F_T$, we have

$$\hat{r} \;=\; r_2\, \xi \,+\, r_3 \eta\,, \quad \text{and} \quad \max\{r_2\,, r_3\} \leq c_3\, \min\{r_2\,, r_3\}\,. \tag{3.31}$$

Lemma 4 *There exists a $C(\widehat{T})$ such that for all $T \in \mathcal{T}_h$*

$$\forall v \in {}_1W^{k+1,p}(T)\,, \qquad \inf_{p\in P_k(\widehat{T})} \|\|\hat{v}+p\|\|_{{}_1W^{k+1,p}(T)} \;\le\; C(\widehat{T})\,\|\|\hat{v}\|\|_{{}_1W^{k+1,p}(T)}\,. \tag{3.32}$$

Proof:
For T of **Type 1**: From (3.28), $\forall\ \ v \in W^{k+1,p}(\widehat{T})$ there exists C_1 such that

$$\inf_{p\in P_k(\widehat{T})} \|v+p\|_{W^{k+1,p}(\widehat{T})} \;\le\; C_1\,|v|_{W^{k+1,p}(\widehat{T})}\,.$$

Now,

$$\begin{aligned}\|\|\hat{v}+p\|\|_{{}_1W^{k+1,p}(T)} &\le r_{max}(T)\|\hat{v}+p\|_{W^{k+1,p}(\widehat{T})} \;\le\; C_1\,r_{max}(T)\,|\hat{v}|_{W^{k+1,p}(\widehat{T})}\\ &\le C_1\,\frac{r_{max}(T)}{r_{min}(T)}\|\|\hat{v}\|\|_{W^{k+1,p}(T)} \;\le\; c_2C_1\,\|\|\hat{v}\|\|_{W^{k+1,p}(T)}\,.\end{aligned} \tag{3.33}$$

For T of **Type 2**: For this case, all the triangles have the same (up to a multiplicative constant) weighted norm on $\widehat{T}$. Hence for all T of this type it follows from (3.28) that there exists a constant C_2 such that (3.32) holds with $C(\widehat{T}) = C_2$.

For T of **Type 3**: Let $\widetilde{T}$ denote the triangle with vertices $S_1(0,0)$, $S_2(1,0)$, $S_3(1,1)$, i.e. $r_2 = r_3 = 1$ in (3.31), and C_3 be given by $\forall\ \ v \in {}_1W^{k+1,p}(\widetilde{T})$

$$\inf_{p\in P_k(\widehat{T})} \|\hat{v}+p\|_{{}_1W^{k+1,p}(\widetilde{T})} \;\le\; C_3\,\|\|\hat{v}\|\|_{{}_1W^{k+1,p}(\widetilde{T})}\,.$$

Assume T has vertices $S_1(0,z_1)$, $S_2(r_2,z_2)$, $S_3(r_3,z_3)$. Then

$$\begin{aligned}\|\|\hat{v}+p\|\|_{{}_1W^{k+1,p}(T)} &\le \max\{r_2,\,r_3\}\|\|\hat{v}+p\|\|_{{}_1W^{k+1,p}(\widetilde{T})} \;\le\; \max\{r_2,\,r_3\}\,C_3|\hat{v}|_{{}_1W^{k+1,p}(\widetilde{T})}\\ &\le C_3\,\frac{\max\{r_2,\,r_3\}}{\min\{r_2,\,r_3\}}\|\|\hat{v}\|\|_{{}_1W^{k+1,p}(T)} \;\le\; c_3C_3\,\|\|\hat{v}\|\|_{{}_1W^{k+1,p}(T)}\,.\end{aligned} \tag{3.34}$$

Finally, with $C(\widehat{T}) = \max\{c_2C_1,\,C_2,\,c_3C_3\}$, the stated result follows.

■

For convenience we assume that $\mathcal{T}_h$ denotes a uniform, regular triangulation of Ω, with characteristic parameter h. The results also hold for a regular triangulation with the error estimates given element by element involving the element parameter h_T.

Corollary 1 *Let $\mathbf{u} \in {}_1H^{k+1}(\Omega)$ and $\rho_h(\mathbf{u})$ be given by (3.14). Then, there exists $C > 0$ such that*

$$\|\mathbf{u} - \rho_h(\mathbf{u})\|_{{}_1L^2(\Omega)} \;\le C\ h^{k+1}\,|\mathbf{u}|_{{}_1H^{k+1}(\Omega)}\,. \tag{3.35}$$

If, in addition $div_{axi}\mathbf{u} \in {}_1H^{k+1}(\Omega)$ and $\Big(\sum_{T\in\mathcal{T}_h}|div_{axi}\rho_h(\mathbf{u})|^2_{{}_1H^{k+1}(T)}\Big)^{1/2} < C_1$, then there exists $C > 0$ such that

$$\|div_{axi}\mathbf{u} - div_{axi}\rho_h(\mathbf{u})\|_{{}_1L^2(\Omega)} \;\le C\ h^{k+1}\,. \tag{3.36}$$

Proof: Estimate (3.35) follows from Lemmas 3 and 4, and the Bramble-Hilbert Lemma [6]. (See also [11], Theorem 3.1.4.) To establish (3.36), using the triangle inequality and Lemma 1, for $T \in \mathcal{T}_h$

$$\begin{aligned}
\|div_{axi}\mathbf{u} \;-\; & div_{axi}\rho_h(\mathbf{u})\|^2_{{}_1L^2(T)} \;\leq \\
& 2\|div_{axi}\mathbf{u} \,-\, \pi_k div_{axi}\rho_h(\mathbf{u})\|^2_{{}_1L^2(T)} \;+\; 2\|div_{axi}\rho_h(\mathbf{u}) \,-\, \pi_k div_{axi}\rho_h(\mathbf{u})\|^2_{{}_1L^2(T)} \\
= \;& 2\|div_{axi}\mathbf{u} \,-\, \pi_k div_{axi}\mathbf{u}\|^2_{{}_1L^2(T)} \;+\; 2\|div_{axi}\rho_h(\mathbf{u}) \,-\, \pi_k div_{axi}\rho_h(\mathbf{u})\|^2_{{}_1L^2(T)} \\
\leq \;& 2\,C\,h^{k+1}\,|div_{axi}\mathbf{u}|^2_{{}_1H^{k+1}(T)} \;+\; 2\,C\,h^{k+1}\,|div_{axi}\rho_h(\mathbf{u})|^2_{{}_1H^{k+1}(T)}\,. \qquad (3.37)
\end{aligned}$$

Summing over the triangles T in $\mathcal{T}_h$ we obtain (3.36).

■

Corollary 2 *Let $\mathbf{u} \in {}_1H^{k+1}(\Omega)$ and $\tilde{\rho}_h(\mathbf{u})$ be given by (3.19). Then, there exists $C > 0$ such that*

$$\|\mathbf{u} \,-\, \tilde{\rho}_h(\mathbf{u})\|_{{}_1L^2(\Omega)} \;\leq C\; h^{k+1}\,|\mathbf{u}|_{{}_1H^{k+1}(\Omega)}\,. \qquad (3.38)$$

If, in addition $div_{axi}\mathbf{u} \in {}_1H^k(\Omega)$ and $\Big(\sum_{T\in\mathcal{T}_h}|div_{axi}\tilde{\rho}_h(\mathbf{u})|^2_{{}_1H^{k+1}(T)}\Big)^{1/2} \;<\; C_1$, then there exists $C > 0$ such that

$$\|div_{axi}\mathbf{u} \,-\, div_{axi}\tilde{\rho}_h(\mathbf{u})\|_{{}_1L^2(\Omega)} \;\leq C\; h^k\,. \qquad (3.39)$$

■

3.1 Grad-Div approximation of (2.13)(2.14)

In order to numerically approximate (2.13)(2.14) we introduce a *grad-div* stabilization into the approximation equations. *For $\gamma > 0$ and $\mathbf{f} \in X^*$ given, determine $(\mathbf{u}_h,\, p_h) \in (X_h \times Q_h)$ satisfying*

$$\begin{aligned}
a(\mathbf{u}_h,\,\mathbf{v}) \;+\; \gamma\int_\Omega div_{axi}(\mathbf{u}_h)\,div_{axi}(\mathbf{v})\,r\,d\mathbf{x} \;-\; b_a(p_h,\,\mathbf{v}) \;&=\; \langle\mathbf{f},\mathbf{v}\rangle_{X^*,X} \quad \forall\mathbf{v}\in X_h\,, \qquad (3.40)\\
b_a(q,\,\mathbf{u}_h) \;&=\; 0\,, \quad \forall q \in Q_h\,. \qquad (3.41)
\end{aligned}$$

Note that from (2.14) $\mathbf{u}$ satisfies

$$\int_\Omega div_{axi}(\mathbf{u}_h)\,div_{axi}(\mathbf{v})\,r\,d\mathbf{x} \;=\; 0\,,\; \forall\mathbf{v}\in X\,. \qquad (3.42)$$

Recently grad-div stabilization has received a good deal of attention for the approximation of fluid flow model by the Navier-Stokes and Stokes equations [20, 21, 19, 16, 10]. For such flows it is well known that the stabilization improves mass conservation and relaxes the effect of the pressure error on the velocity error.

Suppose that the approximation spaces X_h and Q_h are inf-sup stable, i.e. satisfy (3.3). Let

$$Z_h \;:=\; \{\mathbf{v}\in X_h \,:\, b_a(q,\mathbf{v}) = 0\,,\,\forall q\in Q_h\}\,. \qquad (3.43)$$

Then, the existence and unique of the solution to (3.40)(3.41) is equivalent to the existence and uniqueness of $\mathbf{u}_h$ satisfying

$$a_\gamma(\mathbf{u}_h,\, \mathbf{v}) \;:=\; a(\mathbf{u}_h,\, \mathbf{v}) \;+\; \gamma \int_\Omega div_{axi}(\mathbf{u}_h)\, div_{axi}(\mathbf{v})\, r\, d\mathbf{x} \;=\; \langle \mathbf{f}, \mathbf{v}\rangle_{X^*,X} \quad \forall \mathbf{v} \in Z_h\,. \tag{3.44}$$

Observe that

$$(i)\ \text{(Coercivity):}\quad a_\gamma(\mathbf{v}\,,\, \mathbf{v}) \;\geq\; c\|\mathbf{v}\|_X^2\,,\ \text{where}\ \ c = \min\{\nu,\, \gamma\}\,, \tag{3.45}$$

$$(ii)\ \text{(Continuity):}\quad a_\gamma(\mathbf{u}\,,\, \mathbf{v}) \;\leq\; C\|\mathbf{u}\|_X\, \|\mathbf{v}\|_X\,,\ \text{where}\ \ C \,=\, \nu + \gamma\,. \tag{3.46}$$

Theorem 2 *For $\gamma > 0$, there exists a unique solution $(\mathbf{u}_h\,,\, p_h)$ to (3.40)(3.41).*

Proof Properties (3.45)(3.46) guarantee the existence and uniqueness of $\mathbf{u}_h$ satisfying (3.44), and (3.3) then guarantees the existence and uniqueness of p_h satisfying (3.40).

■

Remark: Note that the coercivity of the operator $a_\gamma(\cdot\,,\, \cdot)$ with respect to the X-norm is a result of the added grad-div stabilization term.

For the error bound between $(\mathbf{u}, p)$ satisfying (2.13)(2.14) and $(\mathbf{u}_h\,,\, p_h)$ satsifying (3.40)(3.41) we have the following.

Theorem 3 *(Error Bound) Assume that $(X_h,\, Q_h)$ satisfy (3.3) and that $(\mathbf{u},\, p)$, $(\mathbf{u}_h,\, p_h)$ are given by (2.13)(2.14) and (3.40)(3.41), respectively. Then, there exists a constant $C > 0$ (depending on γ) such that*

$$\|\mathbf{u} \,-\, \mathbf{u}_h\|_X \;+\; \|p \,-\, p_h\|_Q \;\leq\; C\, \left(\inf_{\mathbf{w}_h \in X_h} \|\mathbf{u} \,-\, \mathbf{w}_h\|_X \;+\; \inf_{q_h \in Q_h} \|p \,-\, q_h\|_Q \right)\,. \tag{3.47}$$

Proof: Subtracting (3.44) from (2.13), using 3.42, we obtain

$$a_\gamma(\mathbf{u} \,-\, \mathbf{u}_h,\, \mathbf{v}) \,-\, b_a(p - q,\, \mathbf{v}) \;=\; 0 \quad \forall \mathbf{v} \in Z_h\,, q \in Q_h\,.$$

The error estimate (3.47) is then established in an analogous manner as the standard error analysis for the finite element approximation to Stokes equations [8, 12].

■

3.1.1 Stability of $RT_k^{axi} - discP_k$ and $BDM_k^{axi} - discP_{k-1}$

To establish the stability of approximations to (3.40)(3.41) using $RT_k^{axi} - discP_k$ and $BDM_k^{axi} - discP_{k-1}$ elements, for $k \geq 1$, we use the macro element technique of Stenberg [23, 25], see also [13]. The condition that $k \geq 1$ implies that X_h contains the space of continuous piecewise linear elements.

Lemma 5 *Stenberg's macro element stability criteria given in [25] extends to the $inf-sup$ condition (3.3).*

Proof: The proof follows in an analogous manner to that of Theorem 2.1 in [25]. The existence of an interpolant $\tilde{\mathbf{w}} \in X_h$ to $\mathbf{w}$ such that

$$\left(\sum_{T \in \mathcal{T}_h} h_T^{-2} \|\mathbf{w} - \tilde{\mathbf{w}}\|^2_{{}_1L^2(T)} \; + \; \sum_{e \in \mathcal{E}(\mathcal{T}_h)} h_e^{-1} \int_e |\mathbf{w} - \tilde{\mathbf{w}}|^2 \, r \, ds \right)^{1/2} \; \leq \; C_3 |\mathbf{w}|_{{}_1H^1} \, ,$$

(see (2.12) in [25]), follows from Theorem 1 and Corollary 1 in [3].

■

Remark: The condition that X_h contains the space of continuous piecewise linear elements is used in [3].

Theorem 4 *For $k \geq 1$, with $X_h - Q_h$ given by $RT_k^{axi} - discP_k$ or $BDM_k^{axi} - discP_{k-1}$ the inf-sup stability condition (3.3) is satisfied.*

Proof: We take as the macro element, M, two triangles sharing a common side, i.e. $M = T_1 \cup T_2$, with $e = T_1 \cap T_2$.

$$\begin{aligned} \text{Let } X_{0,M} &= \{\mathbf{v} \in X_h \, : \, \mathbf{v} \cdot \mathbf{n}|_{\partial M} = 0\} \, , \\ Q_M &= \{p|_M \, : \, p \in Q_h\} \, , \\ \text{and } N_M &= \{p \in Q_M \, : \, b_a(p \, , \, \mathbf{v}) = 0 \, , \; \forall \mathbf{v} \in X_{0,M}\} \, . \end{aligned}$$

The stability follows if N_M is one dimensional, consisting of functions which are constant on M.

Note that for $\mathbf{v} \in X_{0,M}$, $p \in N_M$

$$0 \; = \; b_a(p \, , \, \mathbf{v}) \; = \; \int_{T_1} \mathbf{v} \cdot \nabla_a p \, r \, d\mathbf{x} \, + \, \int_{T_2} \mathbf{v} \cdot \nabla_a p \, r \, d\mathbf{x} \, + \, \int_e \mathbf{v} \cdot \mathbf{n} \, [p] \, r \, ds \, , \tag{3.48}$$

where $[p]$ denotes the jump in p along e.

Proceeding as in [26], for $i = 1, 2$, choose $\mathbf{v}_i \in X_{0,M}$ such that its support lies in T_i and all other degrees of freedom vanish except for those given by (3.7)(b), for $X_h = RT_k^{axi}$, or (3.9)(b), for $X_h = BDM_k^{axi}$. From (3.48) it then follows that p is constant on T_1 and T_2, i.e. $p|_{T_1} = c_1$, and $p|_{T_2} = c_2$. Thus, again from (3.48) we have that

$$0 \; = \; (c_1 \, - \, c_2) \int_e \mathbf{v} \cdot \mathbf{n} \, r \, ds \quad \forall \mathbf{v} \in X_{0,M} \, .$$

As from (3.7)(a), or (3.9)(a), $\int_e \mathbf{v} \cdot \mathbf{n} \, r \, ds$ denotes a degree a freedom, then $c_1 = c_2$, i.e. N_M is one dimensional, consisting of functions which are constant on M.

■

To establish the stability of $RT_0^{axi} - discP_0$ we proceed in a similar manner as in [6], pg. 148.

Lemma 6 *The mapping*

$$\pi_0 \, div_{axi} \, : \, RT_0^{axi} \longrightarrow discP_0$$

is surjective.

Proof: Given $f \in discP_0$, let $\breve{f}$ denoting the lifting of f from Ω to $\breve{\Omega}$. Then, we have that there exists $\breve{u} \in H^2(\breve{\Omega}) \cap H_0^1(\breve{\Omega})$ such that $\Delta\breve{u} = \breve{f}$. Set $\breve{\mathbf{q}} := \nabla_{(x,y,z)}\breve{u}$, and let $\mathbf{q}$ denote the reduction of $\breve{\mathbf{q}}$ to Ω. Then,

$$\begin{aligned}\int_T f\, r\, d\mathbf{x} &= \int_T div_{axi}\mathbf{q}\, r\, d\mathbf{x} \\ &= \int_T div_{axi}\rho_T\mathbf{q}\, r\, d\mathbf{x}\,, \text{ (using Lemma 1)} \\ &= \int_T \pi_0\, div_{axi}\rho_T\mathbf{q}\, r\, d\mathbf{x}\,.\end{aligned}$$

Since $\pi_0\, div_{axi}\rho_T\mathbf{q}$ and f are constant on T, then it follows that $\pi_0\, div_{axi}\rho_T\mathbf{q} = f$.

■

Corollary 3 *The approximating pair $(X_h, Q_h) = (RT_0^{axi}, discP_0)$ satisfies the inf-sup condition (3.3).*

Proof: Note that the mapping $discP_0 \longrightarrow RT_0^{axi}$ constructed in the proof of Lemma 6 is bounded. Therefore, from Fortin's criteria, it follows that the inf-sup condition is satisfied.

■

For the approximation to (3.40)(3.41) with (X_h, Q_h) given by $(RT_k^{axi}, discP_k)$, and $(BDM_k^{axi}, discP_{k-1})$, we have the following a priori error estimates.

Corollary 4 *For $(X_h, Q_h) = (RT_k^{axi}, discP_k)$, $\mathbf{u} \in ({}_1H^{k+1}(\Omega))^2$, with $div_{axi}\mathbf{u} \in {}_1H^{k+1}(\Omega)$ and $\Big(\sum_{T\in\mathcal{T}_h} |div_{axi}\rho_h(\mathbf{u})|^2_{{}_1H^{k+1}(T)}\Big)^{1/2} < C_1$, $p \in {}_1H^{k+1}(\Omega)$, satisfying (2.13)(2.14); $(\mathbf{u}_h, p_h) \in (X_h, Q_h)$, satisfying (3.40)(3.41); we have that there exists $C > 0$ such that*

$$\|\mathbf{u} - \mathbf{u}_h\|_X + \|p - p_h\|_{{}_1L^2(\Omega)} \le C\, h^{k+1}\,. \tag{3.49}$$

Proof: From (3.47), using

$$\inf_{q_h\in Q_h} \|p - q_h\|_Q = \inf_{q_h\in Q_h} \|p - q_h\|_{{}_1L^2(\Omega)} \le C\, h^{k+1}\|p\|_{{}_1H^{k+1}(\Omega)}\,,$$

together with Corollary 1 we obtain (3.49).

■

Corollary 5 *For $(X_h, Q_h) = (BDM_k^{axi}, discP_{k-1})$, $\mathbf{u} \in ({}_1H^{k}(\Omega))^2$, with $div_{axi}\mathbf{u} \in {}_1H^{k}(\Omega)$ and $\Big(\sum_{T\in\mathcal{T}_h} |div_{axi}\tilde{\rho}_h(\mathbf{u})|^2_{{}_1H^{k+1}(T)}\Big)^{1/2} < C_1$, $p \in {}_1H^{k}(\Omega)$, satisfying (2.13)(2.14); $(\mathbf{u}_h, p_h) \in (X_h, Q_h)$, satisfying (3.40)(3.41); we have for $k \ge 1$ that there exists $C > 0$ such that*

$$\|\mathbf{u} - \mathbf{u}_h\|_X + \|p - p_h\|_{{}_1L^2(\Omega)} \le C\, h^{k}\,. \tag{3.50}$$

■

3.2 Direct Approximation of (2.13)(2.14)

The analysis presented above for the grad-div approximation of (2.13)(2.14) breaks down for $\gamma = 0$ as, from (3.45), $a_\gamma(\cdot,\cdot)$ is no longer coercive with respect to $\|\cdot\|_X$. To overcome this loss of coercivity with respect to $\|\cdot\|_X$, following the approach of [2, 24], we introduce mesh dependent norms. Let

$$\mathcal{X}_h \;:=\; \{\mathbf{v} \,:\, \mathbf{v} \in {}_1L^2(T),\; \mathbf{v}\cdot\mathbf{n} \in {}_1L^2(e),\; \forall T \in \mathcal{T}_h,\; \forall e \in \mathcal{E}(\mathcal{T}_h),\; \mathbf{v}\cdot\mathbf{n} = 0 \text{ on } \partial\Omega\}, \tag{3.51}$$

and

$$\mathcal{Q}_h \;:=\; \{q \in {}_1L^2_0(T) \,:\, \nabla_a q \in {}_1L^2(T),\; [q] \in {}_1L^2(e),\; \forall T \in \mathcal{T}_h,\; \forall e \in \mathcal{E}(\mathcal{T}_h)\}\,, \tag{3.52}$$

where $[q]|_e(\mathbf{x}) = q^+(\mathbf{x}) - q^-(\mathbf{x})$, with

$$q^\pm(\mathbf{x}) \;=\; \lim_{\epsilon\to 0^\pm} q(\mathbf{x}+\epsilon\mathbf{n})\,,\; \mathbf{x}\in e\,,$$

and $\mathbf{n}$ a specified normal associated with e.

With these spaces we associate the norms

$$\|\mathbf{v}\|_{0,h} \;=\; \left(\sum_{T\in\mathcal{T}_h}\int_T |\mathbf{v}|^2\, r\, d\mathbf{x} \;+\; \sum_{e\in\mathcal{E}(\mathcal{T}_h)} h_e \int_e |\mathbf{v}\cdot\mathbf{n}|^2\, r\, ds\right)^{1/2}, \tag{3.53}$$

$$\|q\|_{1,h} \;=\; \left(\sum_{T\in\mathcal{T}_h}\int_T |\nabla_a q|^2\, r\, d\mathbf{x} \;+\; \sum_{e\in\mathcal{E}(\mathcal{T}_h)} h_e^{-1} \int_e [q]^2\, r\, ds\right)^{1/2}. \tag{3.54}$$

By a scaling argument [2] it is straightforward to show that there exists $c > 0$ such that

$$c\,\|\mathbf{v}\|_{0,h} \;\le\; \|\mathbf{v}\|_{{}_1L^2(\Omega)} \;\le\; \|\mathbf{v}\|_{0,h}\,,\; \forall \mathbf{v}\in\mathcal{X}_h\,, \tag{3.55}$$

and that their exists $C > 0$ such that

$$\|q\|_{1,h} \;\le\; \left(\sum_{T\in\mathcal{T}_h}\int_T |\nabla_a q|^2\, r\, d\mathbf{x} \;+\; h_T^{-2}\int_T q^2\, r\, d\mathbf{x}\right)^{1/2},\; \forall q\in\mathcal{Q}_h\,. \tag{3.56}$$

With respect to the $\|\cdot\|_{0,h}$ and $\|\cdot\|_{1,h}$ norms,

$$a(\mathbf{u}\,,\,\mathbf{v}) \;\le\; \nu\|\mathbf{u}\|_{{}_1L^2(\Omega)}\,\|\mathbf{v}\|_{{}_1L^2(\Omega)} \;\le\; \nu\|\mathbf{u}\|_{0,h}\,\|\mathbf{v}\|_{0,h}\,, \tag{3.57}$$

$$a(\mathbf{u}\,,\,\mathbf{u}) \;\ge\; \nu\|\mathbf{u}\|^2_{{}_1L^2(\Omega)} \;\ge\; c^2\,\nu\|\mathbf{u}\|^2_{0,h}\,, \tag{3.58}$$

$$\begin{aligned} b(q\,,\,\mathbf{v}) \;&=\; \int_\Omega q\,\nabla_a\cdot r\mathbf{v}\, d\mathbf{x} \;=\; \sum_{T\in\mathcal{T}_h}\int_T \mathbf{v}\cdot\nabla_a q\, r\, d\mathbf{x} \;+\; \sum_{e\in\mathcal{E}(\mathcal{T}_h)}\int_e \mathbf{v}\cdot n\,[q]\, r\, ds \\ &\le\; \|\mathbf{v}\|_{0,h}\,\|q\|_{1,h}\,. \end{aligned} \tag{3.59}$$

In view of (3.57)-(3.59), we have that provided $X_h \subset \mathcal{X}_h$, $Q_h \subset \mathcal{Q}_h$, satisfy

$$\inf_{q\in Q_h}\sup_{\mathbf{v}\in X_h} \frac{b(q,\,\mathbf{v})}{\|\mathbf{v}\|_{0,h}\,\|q\|_{1,h}} \;\ge\; \beta\,, \tag{3.60}$$

there exists a unique $(\mathbf{u}_h\,,\,p_h)\in X_h\times Q_h$ satisfying (3.1)(3.2), for all $(\mathbf{v}\,,\,q)\in X_h\times Q_h$, and

$$\|\mathbf{u}-\mathbf{u}_h\|_{{}_1L^2(\Omega)} \;+\; \|p-p_h\|_{1,h} \;\le\; C\left(\inf_{\mathbf{v}\in X_h}\|\mathbf{u}-\mathbf{v}\|_{{}_1L^2(\Omega)} \;+\; \inf_{q\in Q_h}\|p-q\|_{1,h}\right). \tag{3.61}$$

3.2.1 Stability of $RT_k^{axi} - discP_k$ and $BDM_k^{axi} - discP_{k-1}$

Again, in order to show that the approximation pairs $RT_k^{axi} - discP_k$ and $BDM_k^{axi} - discP_{k-1}$ are stable with respect to (3.60), we begin by verifying that the macro element technique of Stenberg also applies to (3.60). In view of

$$c\|\cdot\|_{0,h} \;\le\; \|\cdot\|_{1L^2(\Omega)} \;\le \|\cdot\|_X \;\le\; \|\cdot\|_{1H^1(\Omega)}\,,$$

the issue to be investigated is the influence of the norm $\|\cdot\|_{1,h}$.

Following the notation in [13], assume that for each $\mathcal{T}_h \in (\mathcal{T}_h)_h$ the triangles can be grouped together to form macro elements M_j, $j = 1, \ldots, m$, which form a macro partition, $\mathcal{M}_h$, of $\overline{\Omega}$. Let Π_h denote the projection, with respect to the innerproduct $\langle q,\, p\rangle := \int_\Omega q\, p\, r\, d\mathbf{x}$, from Q_h onto the space

$$Q_h^C := \{q \in Q \,:\, q|_M \text{ is constant } \forall M \in \mathcal{M}_h\}\,. \tag{3.62}$$

Lemma 7 *For $Q_h = discP_0$, $q \in Q_h$, we have that*

$$\|q\|_{1L^2(\Omega)} \;\le\; C\left(\sum_{e\in\mathcal{E}(\mathcal{T}_h)} h_e^{-1}\int_e [q]^2\, r\, ds\right)^{1/2}. \tag{3.63}$$

Proof: First, note the following generalized Poincaré-Friedrichs inequality established by Brenner in [7]. For $\Psi \subset \mathbb{R}^3$, a connected open polyhedral domain, $\mathcal{P}$ a partition of $\overline{\Psi}$ into polyhedra, $S(\mathcal{P},\Psi)$ the set of all the (open) faces common to two subdomains in $\mathcal{P}$, $H^1(\Psi,\mathcal{P}) = \{\zeta \in L^2(\Psi) : \zeta_D = \zeta|_D \in H^1(D),\ \forall D \in \mathcal{P}\}$, then

$$\|\zeta\|^2_{L^2(\Psi)} \;\le\; C\left(\sum_{D\in\mathcal{P}}\int_D |\nabla\zeta|^2\, dx\, dy\, dz \;+\; \sum_{\sigma\in S(\mathcal{P},\Psi)} (diam\,\sigma)^{-1}\,\|\Pi_{0,\sigma}[\sigma]\|^2_{L^2(\sigma)} \;+\; \left(\int_\Psi \zeta\, dx\, dy\, dz\right)^2\right), \tag{3.64}$$

where $\Pi_{0,\sigma}$ denotes the L^2 orthogonal projection from $L^2(\sigma)$ onto $P_0(\sigma)$, the space of constant functions on σ.

By rotation around the symmetry axis, we lift $\Omega \subset \mathbb{R}^2$ to $\breve{\Omega} \subset \mathbb{R}^3$. The triangulation $\mathcal{T}_h$ of Ω induces a partition $\mathcal{P}_R$ of $\breve{\Omega}$, with each triangle $T \in \mathcal{T}_h$ generating a volume of revolution with cross section T. Next, with respect to the parameter τ, we form a refinement of $\mathcal{P}_R$ by dividing the volumes of revolution up with respect to a partition of $[0, 2\pi)$, denoted by $\mathcal{P}_{R,\tau}$. The partition $\mathcal{P}_{R,\tau}$ is not a polyhedral partition of $\breve{\Omega}$ as its elements, with respect to the symmetry axis, have curved front and back faces. Let $\widetilde{\mathcal{P}_{R,\tau}}$ denote the polyhedral partition obtained from $\mathcal{P}_{R,\tau}$ by replacing the curved front and back faces with planar surfaces.

For $D \in \mathcal{P}_{R,\tau}$, let $\tilde{D}$ denote the corresponding element in $\widetilde{\mathcal{P}_{R,\tau}}$, and $m_D = (a, b, c)$ denote the center of gravity of D. We assume that τ is sufficiently small such that m_D lies in D.

For $q \in Q_h$ define two extension to $\breve{\Omega}$ by $\breve{q}(x, y, z) := q((x^2 + y^2)^{1/2}, z)$ and $\tilde{q}|_{\tilde{D}} = \breve{q}(m_D)$. Note

that $\tilde{q} \in H^1(\breve{\Omega}, \widetilde{\mathcal{P}_{R,\tau}})$, and

$$\lim_{\tau\to 0} \|\tilde{q}\|_{L^2(\breve{\Omega})} = \|\breve{q}\|_{L^2(\breve{\Omega})} \tag{3.65}$$

$$\lim_{\tau\to 0} \sum_{\sigma\in S(\widetilde{\mathcal{P}_{R,\tau}},\breve{\Omega})} (diam\,\sigma)^{-1} \|[\tilde{q}]\|^2_{L^2(\sigma)} = \sum_{\sigma\in S(\mathcal{P}_{R,\tau},\breve{\Omega})} (diam\,\sigma)^{-1} \|[\breve{q}]\|^2_{L^2(\sigma)}$$

$$= \sum_{\sigma\in S(\mathcal{P}_R,\breve{\Omega})} (diam\,\sigma)^{-1} \|[\breve{q}]\|^2_{L^2(\sigma)}\,, \tag{3.66}$$

$$\lim_{\tau\to 0} \int_{\breve{\Omega}} \tilde{q}\,dx\,dy\,dz = \int_{\breve{\Omega}} \breve{q}\,dx\,dy\,dz = 0\,. \tag{3.67}$$

Applying (3.64) to $\tilde{q}$, taking the limit as τ goes to zero, and using (3.65)-(3.67) we obtain

$$\|\breve{q}\|^2_{L^2(\breve{\Omega})} \le C \left(\sum_{\sigma\in S(\mathcal{P}_R,\breve{\Omega})} (diam\,\sigma)^{-1} \|[\breve{q}]\|^2_{L^2(\sigma)} \right)^{1/2},$$

from which (3.63) follows.

■

Lemma 8 *Stenberg's macro element stability criteria given in [23] extends to the inf−sup condition (3.60).*

Proof: The extension of Stenberg's macro element criteria [23] to the axisymmetric setting for the Stokes equations is given in [13]. Of the two key lemmas used in the proof, the first lemma (Lemma 1 in [13]) holds for arbitrary norms on X_h and Q_h. The proof of the second lemma requires that, for $q_h^0 \in Q_h$ given, the construction of a $\mathbf{v}^0 \in X$ satisfying

$$\nabla_a \cdot \mathbf{v}^0 + \frac{1}{r} v_r^0 = \Pi_h q_h^0\,, \quad \text{and} \quad \|\mathbf{v}^0\|_X \le \frac{1}{\beta} \|\Pi_h q_h^0\|_Q\,. \tag{3.68}$$

As, from (3.63), $\|\Pi_h q_h^0\|_Q \le C\|\Pi_h q_h^0\|_{1,h}$, and $\|\mathbf{v}^0\|_{0,h} \le C\|\mathbf{v}^0\|_X$ the stated result follows.

■

Theorem 5 *For $k \ge 1$, with $X_h - Q_h$ given by $RT_k^{axi} - discP_k$ or $BDM_k^{axi} - discP_{k-1}$ the inf-sup stability condition (3.60) is satisfied.*

Proof: For $k \ge 1$ $X_h = RT_k^{axi}$ or BDM_k^{axi} contains the space of continuous piecewise (with respect to $\mathcal{T}_h$) polynomials of degree k in each coordinate. Hence, from Lemma 8, the macro element criteria can be applied. For $k \ge 2$ the same argument used in the proof of Theorem 4 can be applied to establish the stability of $X_h - Q_h$. In case $k = 1$ a macro element consisting of two adjacent triangles is not sufficient in order to apply Lemma 8. In this case we must have that the macro elements satisfy: *If γ is the common part of two macro elements then γ is connected and contains at least two edges of triangles in $\mathcal{T}_h$.* (See [14] for an illustration.) Nonetheless, on such macro elements an analogous argument as used in the proof of Theorem 4 can be applied to establish the stability of

$X_h - Q_h$.

■

In order to obtain an optimal error for the $\|\mathbf{u} - \mathbf{u}_h\|_{{}_1L^2(\Omega)}$, and $\|p - p_h\|_{{}_1L^2(\Omega)}$, we require the following additional assumption and lemma.

Additional assumption: Let $\mathbf{z} \in \left({}_1H^2(\Omega)\right)^2$, $s \in {}_1H^2(\Omega)$, $\mathbf{v}_h \in RT_1^{axi}$ or $\mathbf{v}_h \in BDM_2^{axi}$, $q_h \in discP_1$, and $\mathbf{g} := (\mathbf{z} - \mathbf{v}_h)$, $h := (s - q_h)$. Then the solution $(\boldsymbol{\mu}, \xi) \in X \times Q$ of

$$a(\mathbf{w}, \boldsymbol{\mu}) - b_a(\xi, \mathbf{w}) = \langle \mathbf{g}, \mathbf{w} \rangle_{X^*,X} \quad \forall \mathbf{w} \in X\,, \tag{3.69}$$

$$b_a(t, \boldsymbol{\mu}) = \int_\Omega h\, t\, r\, d\mathbf{x}\,, \quad \forall t \in Q\,, \tag{3.70}$$

satisfies $div_{axi}(\boldsymbol{\mu}) \in {}_1H^1(T)$, $\quad \xi \in {}_1H^2(T)\,, \ \ \forall T \in \mathcal{T}_h$ and

$$\left(\sum_{T \in \mathcal{T}_h} |div_{axi}(\boldsymbol{\mu})|^2_{{}_1H^1(T)} + |\xi|^2_{{}_1H^1(T)} + |\xi|^2_{{}_1H^2(T)} \right)^{1/2} \leq C\, \|\mathbf{g}\|_{{}_1L^2(\Omega)} + \|h\|_{{}_1L^2(\Omega)}\,. \tag{3.71}$$

Lemma 9 *For $T \in \mathcal{T}_h$, $f \in {}_1H^1(T)$, there exists $C > 0$ such that*

$$\sum_{e \in \partial T} h_e^{-1} \int_e f^2\, r\, ds \leq C \left(h_T^{-2} \|f\|^2_{{}_1L^2(T)} + |f|^2_{{}_1H^1(T)} \right)\,. \tag{3.72}$$

Proof: The proof follows as in the proof of the Trace Theorem, [6].

■

For the approximations $(\mathbf{u}_h\,, p_h)$ we have the following a priori error estimates.

Corollary 6 *For $\mathbf{u} \in ({}_1H^{k+1}(\Omega))^2$, $p \in {}_1H^{k+1}(\Omega)$, satisfying (2.13)(2.14), $\mathbf{u}_h \in RT_k^{axi} = X_h$, $p_h \in discP_k = Q_h$, satisfying (3.1)(3.2), we have for $k \geq 1$ that there exists $C > 0$ such that*

$$\|\mathbf{u} - \mathbf{u}_h\|_{{}_1L^2(\Omega)} + \|p - p_h\|_{1,h} \leq C\, h^k\,. \tag{3.73}$$

With the additional regularity assumption (3.71),

$$\|\mathbf{u} - \mathbf{u}_h\|_{{}_1L^2(\Omega)} + \|p - p_h\|_{{}_1L^2(\Omega)} \leq C\, h^{k+1}\,. \tag{3.74}$$

Proof: Note that as $k \geq 1$, $p \in C(\Omega)$, From [3], and (3.56)

$$\begin{aligned} \inf_{q \in Q_h} \|p - q\|_{1,h} &\leq C \inf_{q \in Q_h} \left(\sum_{T \in \mathcal{T}_h} \int_T |\nabla_a (p - q)|^2\, r\, d\mathbf{x} + h_T^{-2} \int_T (p - q)^2\, r\, d\mathbf{x} \right)^{1/2} \\ &\leq C\, h^k\, \|p\|_{{}_1H^{k+1}(\Omega)}\,. \end{aligned} \tag{3.75}$$

Estimate (3.73) then follows from (3.75) and (3.35).

To establish (3.74), consider $(\boldsymbol{\mu},\, \xi)$ satisfying (3.69)(3.70) for $\mathbf{g} \,=\, \mathbf{u} - \mathbf{u}_h$, $h \,=\, p - p_h$. With the choices $\mathbf{w} \,=\, \mathbf{u} - \mathbf{u}_h$, $t \,=\, p - p_h$, combining (3.69)(3.70) with (2.13)(2.14) and (3.1)(3.2), we obtain for $(\mathbf{v},\, q) \in X_h \times Q_h$

$$\begin{aligned} & \|\mathbf{u} - \mathbf{u}_h\|^2_{{}_1L^2(\Omega)} \;+\; \|p - p_h\|^2_{{}_1L^2(\Omega)} \\ =\; & a(\mathbf{u} - \mathbf{u}_h,\, \boldsymbol{\mu} - \mathbf{v}) \;-\; b_a(\xi,\, \mathbf{u} - \mathbf{u}_h) \;+\; b_a(p - p_h,\, \mathbf{v}) \;-\; b_a(p - p_h,\, \boldsymbol{\mu}) \;+\; b_a(q, \mathbf{u} - \mathbf{u}_h) \\ =\; & a(\mathbf{u} - \mathbf{u}_h,\, \boldsymbol{\mu} - \mathbf{v}) \;-\; b_a(\xi - q,\, \mathbf{u} - \mathbf{u}_h) \;-\; b_a(p - p_h,\, \boldsymbol{\mu} - \mathbf{v})\,. \end{aligned} \tag{3.76}$$

For each of the terms of the RHS of (3.76):

$$a(\mathbf{u} - \mathbf{u}_h,\, \boldsymbol{\mu} - \mathbf{v}) \;\leq\; \|\mathbf{u} - \mathbf{u}_h\|_{{}_1L^2(\Omega)}\, \|\boldsymbol{\mu} - \mathbf{v}\|_{{}_1L^2(\Omega)} \tag{3.77}$$

$$b_a(p - p_h,\, \boldsymbol{\mu} - \mathbf{v}) \;\leq\; \|p - p_h\|_{{}_1L^2(\Omega)}\, \|div_{axi}(\boldsymbol{\mu} - \mathbf{v})\|_{{}_1L^2(\Omega)} \tag{3.78}$$

$$\begin{aligned} b_a(\xi - q,\, \mathbf{u} - \mathbf{u}_h) \;&=\; \sum_{T\in\mathcal{T}_h} \int_{\partial T} (\mathbf{u} - \mathbf{u}_h)\cdot \mathbf{n}\, (\xi - q)\, r\, ds \;+\; \int_T \nabla_a(\xi - q)\cdot(\mathbf{u} - \mathbf{u}_h)\, r\, d\mathbf{x} \\ &\leq\; C\, \|\mathbf{u} - \mathbf{u}_h\|_{0,h} \left(\sum_{T\in\mathcal{T}_h} h_e^{-1} \int_{\partial T} (\xi - q)^2\, r\, ds \;+\; \int_T |\nabla_a(\xi - q)|^2\, r\, d\mathbf{x} \right)^{1/2} \\ &\leq\; C\, \|\mathbf{u} - \mathbf{u}_h\|_{0,h} \left(\sum_{T\in\mathcal{T}_h} h_T^{-2} \|\xi - q\|^2_{{}_1L^2(T)} \;+\; |\xi - q|^2_{{}_1H^1(T)} \right)^{1/2}. \end{aligned} \tag{3.79}$$

Combining (3.76)-(3.79), using (3.73) and the fact that $(\mathbf{v},\, q) \in X_h \times Q_h$ is arbitrary,

$$\begin{aligned} \|\mathbf{u} - \mathbf{u}_h\|^2_{{}_1L^2(\Omega)} \;+\; & \|p - p_h\|^2_{{}_1L^2(\Omega)} \\ \leq\; & C\, \big(\|\mathbf{u} - \mathbf{u}_h\|_{{}_1L^2(\Omega)} \;+\; \|p - p_h\|_{{}_1L^2(\Omega)} \big)\, \cdot \\ \big(\|\boldsymbol{\mu} - \mathbf{v}\|_{{}_1L^2(\Omega)} \;+\; & \big(\sum_{T\in\mathcal{T}_h} \|div_{axi}(\boldsymbol{\mu} - \mathbf{v})\|^2_{{}_1L^2(T)} \;+\; h_T^{-2} \|\xi - q\|^2_{{}_1L^2(T)} \;+\; |\xi - q|^2_{{}_1H^1(T)} \big)^{1/2} \big) \\ \leq\; & Ch^k \big(\sum_{T\in\mathcal{T}_h} h_T^2 |div_{axi}(\boldsymbol{\mu})|^2_{{}_1H^1(T)} \;+\; h_T^2 |\xi|^2_{{}_1H^1(T)} \;+\; h_T^2 |\xi|^2_{{}_1H^2(T)} \big)^{1/2} \\ \leq\; & Ch^{k+1} \left(\|\mathbf{u} - \mathbf{u}_h\|_{{}_1L^2(\Omega)} \;+\; \|p - p_h\|_{{}_1L^2(\Omega)} \right), \end{aligned} \tag{3.80}$$

where in the last two steps we have used the additional regularity assumption.

■

Similarly, we have the following error estimates when using $(X_h,\, Q_h) \,=\, (BDM_k^{axi},\, discP_{k-1})$.

Corollary 7 *For $\mathbf{u} \in ({}_1H^k(\Omega))^2$, $p \in {}_1H^k(\Omega)$, satisfying (2.13)(2.14), $\mathbf{u}_h \in BDM_k^{axi} \,=\, X_h$, $p_h \in discP_{k-1} \,=\, Q_h$, satisfying (3.1)(3.2), we have for $k \geq 2$ that there exists $C > 0$ such that*

$$\|\mathbf{u} - \mathbf{u}_h\|_{{}_1L^2(\Omega)} \;+\; \|p - p_h\|_{1,h} \;\leq\; C\, h^{k-1}\,. \tag{3.81}$$

With the additional regularity assumption (3.71),

$$\|\mathbf{u} - \mathbf{u}_h\|_{{}_1L^2(\Omega)} \;+\; \|p - p_h\|_{{}_1L^2(\Omega)} \;\leq\; C\, h^k\,. \tag{3.82}$$

■

4 Numerical Results

In this section we present results of numerical experiments for the approximation of (2.13)(2.14) using $RT_k^{axi} - discP_k$, $k = 0, 1, 2$, and $BDM_k^{axi} - discP_{k-1}$, $k = 1, 2$, approximating elements. Two examples are considered. For the first example the true solution for the velocity is a quadratic (vector) function, and the true pressure is a (scalar) quadratic function. The second example is a modification of the Taylor-Green vortex flow problem, a prototypal problem in Navier-Stokes flow approximation.

For the grad-div stabilized approximation, discussed in Section 3.1, $\gamma = 1$ is used in Example 1, and for Example 2 results using $\gamma = 1$, and $\gamma = 10$ are presented. Results from the direct approximation, discussed in Section 3.2, corresponding to $\gamma = 0$, are given in Tables 4.2 and 4.5. In the tables n/a is used to indicate that the theoretical results established in Sections 3.1.1 and 3.2.1 are not applicable.

For both examples we take $\Omega = (0, 1/2) \times (-1/2, 1/2)$, $\Gamma_0 = \{0\} \times [-1/2, 1/2]$, $\Gamma = \partial\Omega \backslash \Gamma_0$.

Example 1
For the true solution we use

$$\mathbf{u}(r, z) = \begin{bmatrix} rz \\ 0.25 - z^2 \end{bmatrix}, \quad \text{and} \quad p(r, z) = rz + 2r + 3z - 2/3\,. \tag{4.1}$$

Note that for the $RT_2^{axi} - discP_2$ approximating elements, $\mathbf{u} \in X_h$ and $p \in Q_h$.

The numerical results are presented in Tables 4.1 and 4.2. An illustration of the computational mesh corresponding to $h = 1/6$ is given in Figure 4.1.

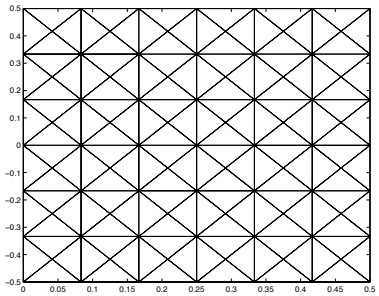

Figure 4.1: Computational mesh corresponding to $h = 1/6$.

Example 2
We consider a modified Taylor-Green vortex flow problem

$$\begin{aligned} \mathbf{u}(r, z) &= \begin{bmatrix} -r\cos(\omega\pi r)\sin(\omega\pi z) \\ -\frac{2}{\omega\pi}\cos(\omega\pi r)\cos(\omega\pi z) + r\sin(\omega\pi r)\cos(\omega\pi z) \end{bmatrix}, \\ p(r, z) &= \sin(\omega\pi z)(-\cos(\omega\pi r) + 2\omega\pi r\sin(\omega\pi r))\,. \end{aligned}$$

The computations are performed for $\omega = 1$. A plot of the velocity field $\mathbf{u}$, and the pressure p, is given in Figures 4.2 and 4.3, respectively.

The numerical results are presented in Tables 4.3, 4.4, and 4.5.

h	$\|\mathbf{u}-\mathbf{u}_h\|_{1L^2(\Omega)}$	Cvg. rate	$\|\mathbf{u}-\mathbf{u}_h\|_X$	Cvg. rate	$\|p-p_h\|_Q$	Cvg. rate
$\gamma=1 \quad X_h=RT_0^{axi} \quad Q_h=discP_0$						
1/4	1.629E-2	1.01	2.020E-2	0.94	5.151E-2	1.00
1/6	1.083E-2	1.00	1.382E-2	0.93	3.432E-2	1.00
1/8	8.117E-3	1.00	1.058E-2	0.93	2.573E-2	1.00
1/10	6.496E-3	1.00	8.606E-3	0.92	2.059E-2	1.00
1/12	5.415E-3		7.271E-3		1.715E-2	
Pred.		1.0		1.0		1.0
$\gamma=1 \quad X_h=RT_1^{axi} \quad Q_h=discP_1$						
1/4	7.279E-4	1.97	1.112E-3	1.92	1.843E-4	2.00
1/6	3.272E-4	1.98	5.111E-4	1.93	8.194E-5	2.00
1/8	1.852E-4	1.99	2.937E-4	1.93	4.609E-5	2.00
1/10	1.188E-4	2.00	1.909E-4	1.93	2.950E-5	2.00
1/12	8.246E-5		1.343E-4		2.048E-5	
Pred.		2.0		2.0		2.0
$\gamma=1 \quad X_h=RT_2^{axi} \quad Q_h=discP_2$						
1/4	1.531E-13		1.585E-13		1.521E-14	
1/6	4.892E-13		5.128E-13		2.181E-14	
1/8	2.614E-12		2.701E-12		3.296E-14	
1/10	5.398E-12		5.592E-12		1.306E-13	
1/12	1.438E-11		1.451E-11		1.580E-13	
Pred.						
$\gamma=1 \quad X_h=BDM_1^{axi} \quad Q_h=discP_0$						
1/4	2.279E-2	0.90	4.107E-2	0.90	5.137E-2	1.00
1/6	1.582E-2	0.93	2.846E-2	0.94	3.424E-2	1.00
1/8	1.212E-2	0.94	2.174E-2	0.95	2.567E-2	1.00
1/10	9.824E-3	0.95	1.757E-2	0.96	2.054E-2	1.00
1/12	8.259E-3		1.474E-2		1.711E-2	
Pred.		1.0		1.0		1.0
$\gamma=1 \quad X_h=BDM_2^{axi} \quad Q_h=discP_1$						
1/4	8.300E-5	1.99	1.420E-4	1.99	1.835E-4	2.00
1/6	3.704E-5	2.00	6.342E-5	1.99	8.170E-5	2.00
1/8	2.086E-5	2.00	3.574E-5	2.00	4.599E-5	2.00
1/10	1.336E-5	2.00	2.289E-5	2.00	2.944E-5	2.00
1/12	9.282E-6		1.591E-5		2.045E-5	
Pred.		2.0		2.0		2.0

Table 4.1: Example 1, $\gamma = 1$.

5 Conclusion

In this paper we establish the stability and a priori error estimates for the $RT_k^{axi} - discP_k$ and $BDM_k^{axi} - discP_{k-1}$ approximating pairs for axisymmetric Darcy flow. The numerical computations confirm the predicted rates of convergence for the approximation errors.

h	$\|\mathbf{u}-\mathbf{u}_h\|_{1L^2(\Omega)}$	Cvg. rate	$\|p-p_h\|_Q$	Cvg. rate	$\|p-p_h\|_{1,h}$	Cvg. rate
$\gamma=0$ $X_h=RT_0^{axi}$ $Q_h=discP_0$						
1/4	1.260E-2	1.05	5.140E-2	1.00	1.874E+0	-0.01
1/6	8.225E-3	1.03	3.424E-2	1.00	1.880E+0	-0.01
1/8	6.121E-3	1.02	2.568E-2	1.00	1.884E+0	0.00
1/10	4.879E-3	1.01	2.054E-2	1.00	1.886E+0	0.00
1/12	4.058E-3		1.712E-2		1.887E+0	
Pred.		n/a		n/a		n/a
$\gamma=0$ $X_h=RT_1^{axi}$ $Q_h=discP_1$						
1/4	6.670E-4	2.00	1.839E-4	2.00	1.765E-2	0.99
1/6	2.969E-4	2.00	8.178E-5	2.00	1.182E-2	0.99
1/8	1.671E-4	2.00	4.601E-5	2.00	8.880E-3	0.99
1/10	1.070E-4	2.00	2.945E-5	2.00	7.113E-3	1.00
1/12	7.433E-5		2.046E-5		5.932E-3	
Pred.		2.0		2.0		1.0
$\gamma=0$ $X_h=RT_2^{axi}$ $Q_h=discP_2$						
1/4	4.254E-14		1.276E-14		1.227E-12	
1/6	1.371E-13		1.279E-14		1.836E-12	
1/8	5.344E-13		1.384E-14		2.561E-12	
1/10	4.017E-13		1.326E-14		3.197E-12	
1/12	2.893E-12		2.340E-14		4.203E-12	
Pred.						
$\gamma=0$ $X_h=BDM_1^{axi}$ $Q_h=discP_0$						
1/4	1.295E-1	0.74	5.156E-2	1.00	1.862E+0	-0.02
1/6	9.593E-2	0.79	3.432E-2	1.00	1.874E+0	-0.01
1/8	7.636E-2	0.82	2.571E-2	1.00	1.879E+0	-0.01
1/10	6.360E-2	0.84	2.056E-2	1.00	1.883E+0	-0.01
1/12	5.461E-2		1.713E-2		1.885E+0	
Pred.		n/a		n/a		n/a
$\gamma=0$ $X_h=BDM_2^{axi}$ $Q_h=discP_1$						
1/4	4.771E-4	1.90	1.836E-4	2.00	1.765E-2	0.99
1/6	2.208E-4	1.91	8.173E-5	2.00	1.182E-2	0.99
1/8	1.276E-4	1.91	4.600E-5	2.00	8.880E-3	0.99
1/10	8.329E-5	1.91	2.945E-5	2.00	7.113E-3	1.00
1/12	5.874E-5		2.045E-5		5.932E-3	
Pred.		2.0		2.0		1.0

Table 4.2: Example 1, $\gamma = 0$.

References

[1] R.A. Adams and J.J.F. Fournier. *Sobolev spaces*, volume 140 of *Pure and Applied Mathematics (Amsterdam)*. Elsevier/Academic Press, Amsterdam, second edition, 2003.

[2] I. Babuška, J. Osborn, and J. Pitkäranta. Analysis of mixed methods using mesh dependent norms. *Math. Comp.*, 35(152):1039–1062, 1980.

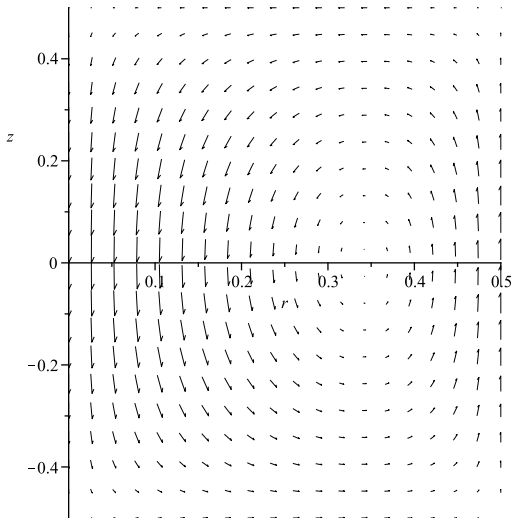

Figure 4.2: Plot of the velocity flow field $\mathbf{u}$.

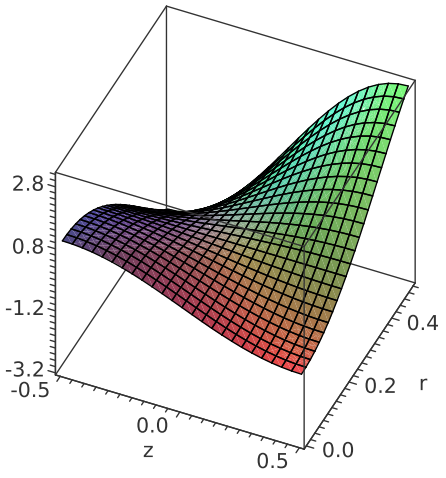

Figure 4.3: Plot of the pressure function p.

[3] Z. Belhachmi, C. Bernardi, and S. Deparis. Weighted Clément operator and application to the finite element discretization of the axisymmetric Stokes problem. *Numer. Math.*, 105(2):217–247, 2006.

[4] Z. Belhachmi, C. Bernardi, S. Deparis, and F. Hecht. A truncated Fourier/finite element discretization of the Stokes equations in an axisymmetric domain. *Math. Models Methods Appl. Sci.*, 16(2):233–263, 2006.

[5] C. Bernardi, M. Dauge, and Y. Maday. *Spectral methods for axisymmetric domains*, volume 3 of *Series in Applied Mathematics (Paris)*. Gauthier-Villars, 1999. Numerical algorithms and tests due to Mejdi Azaïez.

[6] D. Braess. *Finite elements*. Cambridge University Press, 2 edition, 2001. Theory, fast solvers, and applications in solid mechanics; Translated from the German by Larry L. Schumaker.

[7] S.C. Brenner. Poincaré-Friedrichs inequalities for piecewise H^1 functions. *SIAM J. Numer. Anal.*, 41(1):306–324 (electronic), 2003.

[8] S.C. Brenner and L.R. Scott. *The mathematical theory of finite element methods*, volume 15 of *Texts in Applied Mathematics*. Springer-Verlag, New York, second edition, 2002.

[9] F. Brezzi and M. Fortin. *Mixed and hybrid finite element methods*. Springer-Verlag, New York, 1991.

h	$\|\mathbf{u}-\mathbf{u}_h\|_{1L^2(\Omega)}$	Cvg. rate	$\|\mathbf{u}-\mathbf{u}_h\|_X$	Cvg. rate	$\|p-p_h\|_Q$	Cvg. rate
$\gamma=1 \quad X_h=RT_0^{axi} \quad Q_h=discP_0$						
1/4	3.553E-2	1.02	3.993E-2	0.89	8.086E-2	1.00
1/6	2.348E-2	1.03	2.788E-2	0.89	5.383E-2	1.00
1/8	1.748E-2	1.02	2.158E-2	0.89	4.035E-2	1.00
1/10	1.391E-2	1.02	1.768E-2	0.89	3.227E-2	1.00
1/12	1.155E-2		1.502E-2		2.689E-2	
Pred.		1.0		1.0		1.0
$\gamma=1 \quad X_h=RT_1^{axi} \quad Q_h=discP_1$						
1/4	2.222E-3	2.04	2.862E-3	1.97	6.423E-3	2.01
1/6	9.705E-4	2.04	1.288E-3	1.96	2.848E-3	2.00
1/8	5.403E-4	2.03	7.324E-4	1.96	1.601E-3	2.00
1/10	3.432E-4	2.03	4.729E-4	1.96	1.024E-3	2.00
1/12	2.369E-4		3.309E-4		7.112E-4	
Pred.		2.0		2.0		2.0
$\gamma=1 \quad X_h=RT_2^{axi} \quad Q_h=discP_2$						
1/4	1.162E-4	3.04	1.591E-4	2.93	3.779E-4	3.01
1/6	3.383E-5	3.02	4.855E-5	2.93	1.115E-4	3.01
1/8	1.418E-5	3.02	2.091E-5	2.93	4.697E-5	3.00
1/10	7.224E-6	3.03	1.087E-5	2.93	2.403E-5	3.00
1/12	4.161E-6		6.367E-6		1.390E-5	
Pred.		3.0		3.0		3.0
$\gamma=1 \quad X_h=BDM_1^{axi} \quad Q_h=discP_0$						
1/4	3.567E-2	0.90	5.300E-2	0.83	8.033E-2	1.00
1/6	2.476E-2	0.93	3.785E-2	0.88	5.350E-2	1.00
1/8	1.897E-2	0.94	2.937E-2	0.91	4.011E-2	1.00
1/10	1.537E-2	0.95	2.397E-2	0.93	3.208E-2	1.00
1/12	1.292E-2		2.024E-2		2.673E-2	
Pred.		1.0		1.0		1.0
$\gamma=1 \quad X_h=BDM_2^{axi} \quad Q_h=discP_1$						
1/4	2.793E-3	1.87	4.245E-3	1.85	6.423E-3	2.01
1/6	1.309E-3	1.91	2.008E-3	1.90	2.848E-3	2.00
1/8	7.560E-4	1.93	1.164E-3	1.92	1.601E-3	2.00
1/10	4.917E-4	1.94	7.581E-4	1.94	1.024E-3	2.00
1/12	3.452E-4		5.327E-4		7.112E-4	
Pred.		2.0		2.0		2.0

Table 4.3: Example 2, $\gamma = 1$.

[10] M.A. Case, V.J. Ervin, A. Linke, and L.G. Rebholz. A connection between Scott-Vogelius and grad-div stabilized Taylor-Hood FE approximations of the Navier-Stokes equations. *SIAM J. Numer. Anal.*, 49:1461–1481, 2011.

[11] P.G. Ciarlet. *The Finite Element Method for Elliptic Problems.* North-Holland, Amsterdam, 1978.

h	$\|\mathbf{u}-\mathbf{u}_h\|_{1\,L^2(\Omega)}$	Cvg. rate	$\|\mathbf{u}-\mathbf{u}_h\|_X$	Cvg. rate	$\|p-p_h\|_Q$	Cvg. rate
$\gamma = 10$ $X_h = RT_0^{axi}$ $Q_h = discP_0$						
1/4	4.705E-2	0.86	4.773E-2	0.83	8.139E-2	1.00
1/6	3.318E-2	0.89	3.409E-2	0.85	5.419E-2	1.00
1/8	2.569E-2	0.91	2.668E-2	0.87	4.062E-2	1.00
1/10	2.098E-2	0.92	2.199E-2	0.88	3.249E-2	1.00
1/12	1.773E-2		1.874E-2		2.707E-2	
Pred.		1.0		1.0		1.0
$\gamma = 10$ $X_h = RT_1^{axi}$ $Q_h = discP_1$						
1/4	3.310E-3	2.03	3.546E-3	1.98	6.432E-3	2.01
1/6	1.451E-3	2.04	1.586E-3	1.99	2.851E-3	2.00
1/8	8.062E-4	2.03	8.944E-4	1.98	1.602E-3	2.00
1/10	5.120E-4	2.03	5.747E-4	1.98	1.025E-3	2.00
1/12	3.539E-4		4.009E-4		7.114E-4	
Pred.		2.0		2.0		2.0
$\gamma = 10$ $X_h = RT_2^{axi}$ $Q_h = discP_2$						
1/4	1.912E-4	3.01	2.064E-4	2.95	3.782E-4	3.01
1/6	5.650E-5	3.03	6.230E-5	2.97	1.116E-4	3.01
1/8	2.362E-5	3.02	2.649E-5	2.97	4.699E-5	3.00
1/10	1.203E-5	3.01	1.367E-5	2.96	2.404E-5	3.00
1/12	6.943E-6		7.970E-6		1.391E-5	
Pred.		3.0		3.0		3.0
$\gamma = 10$ $X_h = BDM_1^{axi}$ $Q_h = discP_0$						
1/4	1.839E-2	0.99	1.924E-2	0.97	8.032E-2	1.00
1/6	1.232E-2	0.99	1.297E-2	0.98	5.350E-2	1.00
1/8	9.260E-3	1.00	9.780E-3	0.99	4.011E-2	1.00
1/10	7.416E-3	1.00	7.848E-3	0.99	3.208E-2	1.00
1/12	6.183E-3		6.554E-3		2.673E-2	
Pred.		1.0		1.0		1.0
$\gamma = 10$ $X_h = BDM_2^{axi}$ $Q_h = discP_1$						
1/4	1.385E-3	1.98	1.460E-3	1.96	6.423E-3	2.01
1/6	6.207E-4	1.99	6.587E-4	1.97	2.848E-3	2.00
1/8	3.505E-4	1.99	3.733E-4	1.98	1.601E-3	2.00
1/10	2.248E-4	1.99	2.400E-4	1.98	1.024E-3	2.00
1/12	1.563E-4		1.672E-4		7.112E-4	
Pred.		2.0		2.0		2.0

Table 4.4: Example 2, $\gamma = 10$.

[12] A. Ern and J.-L. Guermond. *Theory and practice of finite elements*, volume 159 of *Applied Mathematical Sciences*. Springer-Verlag, New York, 2004.

[13] V.J. Ervin and E.W. Jenkins. Stenberg's sufficiency condition for axisymmetric Stokes flow. Technical report, Dept. Math. Sci., Clemson University, 2011. `http://www.clemson.edu/ces/math/technical_reports/ervin.axisym_sten.pdf`.

h	$\|\mathbf{u}-\mathbf{u}_h\|_{1L^2(\Omega)}$	Cvg. rate	$\|p-p_h\|_Q$	Cvg. rate	$\|p-p_h\|_{1,h}$	Cvg. rate
$\gamma=0$ $X_h=RT_0^{axi}$ $Q_h=discP_0$						
1/4	2.387E-2	1.18	8.039E-2	1.00	3.529E+0	-0.01
1/6	1.478E-2	1.09	5.352E-2	1.00	3.547E+0	-0.01
1/8	1.081E-2	1.05	4.012E-2	1.00	3.553E+0	0.00
1/10	8.555E-3	1.03	3.209E-2	1.00	3.557E+0	0.00
1/12	7.088E-3		2.673E-2		3.559E+0	
Pred.		n/a		n/a		n/a
$\gamma=0$ $X_h=RT_1^{axi}$ $Q_h=discP_1$						
1/4	6.495E-3	1.96	6.425E-3	2.01	4.981E-1	1.00
1/6	2.933E-3	1.98	2.849E-3	2.00	3.327E-1	1.00
1/8	1.658E-3	1.99	1.601E-3	2.00	2.497E-1	1.00
1/10	1.064E-3	1.99	1.024E-3	2.00	1.999E-1	1.00
1/12	7.398E-4		7.112E-4		1.666E-1	
Pred.		2.0		2.0		1.0
$\gamma=0$ $X_h=RT_2^{axi}$ $Q_h=discP_2$						
1/4	3.505E-4	3.03	3.780E-4	3.01	4.603E-2	1.99
1/6	1.025E-4	3.02	1.115E-4	3.01	2.054E-2	1.99
1/8	4.302E-5	3.01	4.697E-5	3.00	1.157E-2	2.00
1/10	2.198E-5	3.01	2.403E-5	3.00	7.410E-3	2.00
1/12	1.270E-5		1.390E-5		5.148E-3	
Pred.		3.0		3.0		2.0
$\gamma=0$ $X_h=BDM_1^{axi}$ $Q_h=discP_0$						
1/4	1.095E-1	0.77	8.037E-2	1.00	3.523E+0	-0.01
1/6	8.006E-2	0.81	5.351E-2	1.00	3.543E+0	-0.01
1/8	6.343E-2	0.83	4.011E-2	1.00	3.551E+0	-0.01
1/10	5.266E-2	0.85	3.208E-2	1.00	3.555E+0	0.00
1/12	4.509E-2		2.673E-2		3.558E+0	
Pred.		n/a		n/a		n/a
$\gamma=0$ $X_h=BDM_2^{axi}$ $Q_h=discP_1$						
1/4	1.381E-2	1.87	6.426E-3	2.01	4.982E-1	1.00
1/6	6.474E-3	1.90	2.849E-3	2.00	3.327E-1	1.00
1/8	3.753E-3	1.91	1.601E-3	2.00	2.498E-1	1.00
1/10	2.452E-3	1.92	1.024E-3	2.00	1.999E-1	1.00
1/12	1.729E-3		7.112E-4		1.666E-1	
Pred.		2.0		2.0		1.0

Table 4.5: Example 2, $\gamma = 0$.

[14] M.D. Gunzburger. *Finite element methods for viscous incompressible flows.* Computer Science and Scientific Computing. Academic Press Inc., Boston, MA, 1989.

[15] R.H.W. Hoppe. Finite Element Methods – Course Notes (Chapter 7). Technical report, Department of Mathematics, University of Houston, 2005. `http://www.math.uh.edu/~rohop/spring_05/downloads/Chapter7.pdf`.

[16] W. Layton, C. Manica, M. Neda, M.A. Olshanskii, and L. Rebholz. On the accuracy of the rotation form in simulations of the Navier-Stokes equations. *J. Comput. Phys.*, 228(5):3433–3447, 2009.

[17] Y.-J. Lee and H. Li. On stability, accuracy, and fast solvers for finite element approximations of the axisymmetric Stokes problem by Hood-Taylor elements. *SIAM J. Numer. Anal.*, 49(2):668–691, 2011.

[18] H. Li. Finite element analysis for the axisymmetric Laplace operator on polygonal domains. *J. Comput. Appl. Math.*, 235(17):5155–5176, 2011.

[19] M. Olshanskii, G. Lube, T. Heister, and J. Löwe. Grad-div stabilization and subgrid pressure models for the incompressible Navier-Stokes equations. *Comp. Meth. Appl. Mech. Eng.*, 198:3975–3988, 2009.

[20] M.A. Olshanskii. A low order Galerkin finite element method for the Navier-Stokes equations of steady incompressible flow: A stabilization issue and iterative methods. *Comp. Meth. Appl. Mech. Eng.*, 191:5515–5536, 2002.

[21] M.A. Olshanskii and A. Reusken. Grad-Div stabilization for the Stokes equations. *Math. Comp.*, 73:1699–1718, 2004.

[22] V. Ruas. Mixed finite element methods with discontinuous pressures for the axisymmetric Stokes problem. *ZAMM Z. Angew. Math. Mech.*, 83(4):249–264, 2003.

[23] R. Stenberg. Analysis of mixed finite elements methods for the Stokes problem: A unified approach. *Math. Comp.*, 42:9–23, 1984.

[24] R. Stenberg. On the construction of optimal mixed finite element methods for the linear elasticity problem. *Numer. Math.*, 48(4):447–462, 1986.

[25] R. Stenberg. Error analysis of some finite element methods for the Stokes problem. *Math. Comp.*, 54(190):495–508, 1990.

[26] R. Stenberg. A nonstandard mixed finite element family. *Numer. Math.*, 115(1):131–139, 2010.